Palaeogeography, Palaeoclimatology, Palaeoecology 681 (2026) 113352

Contents lists available at ScienceDirect

Palaeogeography, Palaeoclimatology, Palaeoecology

journal homepage: www.elsevier.com/locate/palaeo

Pollen transport to deep-marine environments: Considerations for reconstructing past vegetation from marine sediment cores

Laura S. McDonald [a,*], Lorna J. Strachan [a], Katherine Holt [b], Adam D. McArthur [c], Anthony E. Shorrock [a], Martin P. Crundwell [a], Katharina Pank [d], Madison Clarke [e], Adam Woodhouse [f], Davide Gamboa [g,h], Jenni L. Hopkins [e], Matt S. McGlone [i], Helen C. Bostock [j]

[a] School of Environment, Waipapa Taumata Rau-University of Auckland, 23 Symonds Street, Auckland-Tāmaki Makaurau, 1142, Aotearoa, New Zealand
[b] School of Agriculture and Environment, Te Kunenga ki Pūrehuroa-Massey University, AgHort Building Manawatū campus, Palmerston North-Te Papaioea, 4474, Aotearoa, New Zealand
[c] School of Earth and Environment, University of Leeds, Earth and Environment building, Leeds, LS2 9JT, UK
[d] GEOMAR Helmholtz Centre for Ocean Research Kiel, Wischhofstraße 1-3, Kiel, 24148, Germany
[e] School of Geography, Environment and Earth Sciences, Te Herenga Waka-Victoria University of Wellington, Cotton Building, Kelburn Parade, Wellington-Te Whanganui-a-Tara, 6012, Aotearoa, New Zealand
[f] School of Earth Sciences, University of Bristol, Beacon House, Queens Road, Bristol, BS8 1QU, UK
[g] Department of Geosciences, University of Aveiro, Campus de Santiago, Aveiro, 3810-193, Portugal
[h] CESAM, University of Aveiro, Campus de Santiago, Aveiro, 3810-193, Portugal
[i] Manaaki Whenua Landcare Research, 76 Gerald Street, Lincoln, 7608, Aotearoa, New Zealand
[j] School of the Environment, University of Queensland, St Lucia, Brisbane, 4067, Australia

ARTICLE INFO

Editor: H. Falcon-Lang

Dataset link: https://doi.org/10.5281/zenodo.16623457

Keywords:
Palynology
Palaeovegetation
Palaeoclimate
Turbidites
Aotearoa-New Zealand
IODP

ABSTRACT

Deep-marine sedimentary records provide a unique opportunity to investigate long-term vegetation changes in response to climate through pollen analysis. In contrast to pollen records from terrestrial sites which capture a local vegetation signature, deep-marine records typically capture a regional vegetation signature, with pollen often taking long and complex transport pathways before depositing on the seafloor. To use deep-marine pollen records to their full potential, we need to understand how pollen is reaching deep-marine sites and whether different transport processes (i.e. ocean currents or gravity flows) impact or bias the final palaeovegetation record. We compare three deep-marine pollen records from offshore eastern Aotearoa-New Zealand from different depths, proximities from land, and sedimentary settings to understand whether these different factors influence the final palaeovegetation records. We focus on the glacial–interglacial transitions from Marine Isotope Stages 6-5 and 2-1, and present a new 135 ka pollen record from the turbidite-dominated sediment core IODP-U1520D. We find that pollen assemblages in the three cores show consistent changes over glacial–interglacial cycles, with pollen assemblages showing greater similarities in interglacial periods and varying during glacial periods. The general consistency in pollen assemblages is surprising given the vastly different nature of the three sediment cores and shows that deep-marine records, including fine-grained turbidite-dominated records from active margins, can yield reliable palaeovegetation records.

1. Introduction

Deep-marine sedimentary records provide an opportunity to create long, continuous, and reliably dated records of past vegetation by analysing the pollen archived in the sediments (Dupont, 1999; Sánchez-Goñi et al., 2018). Globally, there are limited terrestrial pollen records that extend further than the previous interglacial (Marine Isotope Stage 5e), due to continents being a mostly erosive surface, with limited basins where sediment can accumulate to cover multiple glacial–interglacial cycles (Hooghiemstra, 2023). After the discovery that pollen accumulates alongside sediments in deep-marine basins, many long pollen records have been created globally, showing how vegetation has responded to large-scale changes in climate (Hooghiemstra et al., 1992; Lyle et al., 2001; Heusser et al., 2006; Igarashi and Oba, 2006; González et al., 2008; Dupont, 2011; Sánchez-Goñi et al., 2016, 2018). In Aotearoa-New Zealand, there are just a handful of continuous (Newnham, 1992; Shulmeister et al., 2001; Vandergoes

* Corresponding author.
E-mail address: laura.mcdonald@auckland.ac.nz (L.S. McDonald).

https://doi.org/10.1016/j.palaeo.2025.113352
Received 30 June 2025; Received in revised form 31 July 2025; Accepted 14 October 2025
Available online 17 October 2025

et al., 2005; Alloway et al., 2007; Newnham et al., 2007a,b) and discontinuous (McGlone and Topping, 1983; McGlone et al., 1984; Mildenhall, 1995; Newnham and Alloway, 2004; Vandergoes et al., 2013; Newnham et al., 2017; Piva et al., 2023) vegetation records from terrestrial sediment cores that extend through, and beyond, the most recent glacial period (Newnham et al., 1999; Alloway et al., 2007; Barrell et al., 2013). Of the few terrestrial records from Aotearoa-New Zealand that span older glacial–interglacial cycles, age control is often limited (Newnham et al., 1999) due to the 55 ka maximum of radiocarbon dating (Guilderson et al., 2005; Heaton et al., 2020; Li et al., 2021). In contrast, marine sediments can be dated beyond the radiocarbon dating limit by comparing the stable isotope $\delta^{18}O$ from benthic foraminifera to global benthic stacks (Lisiecki and Raymo, 2005), providing an understanding of how vegetation has responded to changes in climate in deeper time (Hooghiemstra et al., 1992; Heusser and Van de Geer, 1994; Kershaw et al., 2003; Mildenhall et al., 2004; Kershaw and Kaars, 2006; Dupont, 2011; Sánchez-Goñi et al., 2016). While deep-marine sediment cores offer clear advantages for reconstructing past vegetation over multiple glacial–interglacial cycles, interpreting the pollen record is often more complex than for terrestrial records (Hooghiemstra et al., 1992; Dupont, 1999; Sánchez-Goñi et al., 2018). In terrestrial records, such as lakes, the source-to-sink path for pollen is relatively straightforward as it is typically sourced from local vegetation adjacent to the site, whereas deep-marine pollen records reflect regional vegetation patterns, as pollen may travel from various hinterland sources before being deposited in the deep ocean (Hooghiemstra et al., 1992; Heusser and Van de Geer, 1994; Mildenhall, 2003; Mildenhall et al., 2004; Dupont, 2011; Sánchez-Goñi et al., 2018). It typically takes pollen longer to reach deep-marine sites, with the potential to be reworked multiple times along transport pathways, which may include a combination of wind (Mildenhall, 1976; Scott and van Zinderen Barker Sr, 1985; Zwier et al., 2022), water (Zhu et al., 2003; Moss et al., 2005; Ryan et al., 2016), and gravity flow transport (McArthur et al., 2017; Vieira and Jolley, 2020; Jolley et al., 2022; McDonald et al., 2024). The long and complex transport pathways that pollen follows to reach a deep-marine site also introduce taphonomic biases into marine pollen records, as certain taxa may be preferentially transported by wind and water (Mildenhall, 1976; Heusser and Balsam, 1977; Holmes, 1990; Montade et al., 2011; McGann, 2018). To use deep-marine pollen records to their full potential to reconstruct vegetation over multiple glacial–interglacial cycles, we need to thoroughly understand how different pollen transport pathways and processes could impact deep-marine pollen records and interpretations of past vegetation.

Here we investigate the complexities of pollen transport and deposition in both proximal and distal deep-marine settings by comparing three deep-marine pollen records from different marine sedimentary settings from offshore eastern Aotearoa-New Zealand: P69/Marion Dufresne(MD)97-2121 (McGlone, 2001; Carter and Manighetti, 2006) positioned on the continental slope, dominated by fine-grained sedimentation; International Ocean Discovery Program (IODP)U1520D (Barnes et al., 2019) positioned in a deep-marine trough dominated by turbidite sediments; and Ocean Drilling Program (ODP)1123B (Carter et al., 1999; Mildenhall et al., 2004), a distal core >1000 km offshore, dominated by carbonate ooze (Fig. 1). We integrate pollen records from these three sites to determine the relative importance of differences in ocean currents, sedimentary processes, and distance from pollen sources in influencing the palaeovegetation records preserved across these different marine settings. We have targeted the two most recent glacial–interglacial cycles, primarily focusing on the glacials Marine Isotope Stage (MIS) 6 and 2 and the interglacials MIS 5e and 1, because this is a time when global climate underwent major changes which influenced the vegetation in Aotearoa-New Zealand, which are documented in terrestrial pollen records, albeit fragmented (McGlone and Topping, 1983; McGlone et al., 1984; Newnham, 1992; Mildenhall, 1995; Shulmeister et al., 2001; Newnham and Alloway, 2004; Vandergoes et al., 2005; Alloway et al., 2007; Newnham et al., 2007a,b, 2013).

The location of the three sediment cores off the east coast of Aotearoa-New Zealand means that pollen and sediment contributing to the records were likely sourced from both Te Waipounamu-South Island and/or Te Ika-a-Māui-North Island (Fig. 1; McGlone, 2001; Mildenhall, 2003; Mildenhall et al., 2004; Orpin, 2004; Parra et al., 2012; Hayward et al., 2022; Underwood, 2022; Woodhouse et al., 2024). The modern North and South Island of Aotearoa-New Zealand exhibit a diverse range of vegetation communities, spanning native communities (i.e. podocarp-hardwood forests, beech forests, shrublands, and grassland; Wardle and P, 1991; Walker et al., 2006) to introduced forests (i.e. *Pinus radiata*; Wilmshurst, 1997; Elliot et al., 2003; Star, 2008). Terrestrial pollen records indicate that before human arrival in Aotearoa-New Zealand (~1250 AD, Wilmshurst et al., 2008), the vegetation during interglacial periods was predominantly composed of podocarp-hardwood forests, with some beech forest at higher elevations (~800–1300 m; Newnham and Lowe, 2000; Alloway et al., 2007; Barrell et al., 2013; Schindler et al., 2021). In glacial periods, shrub and grass communities expanded to cover much of the central North Island and northern South Island as the cooler temperatures caused podocarp-hardwood communities to contract (McGlone, 1985; McGlone et al., 2010; Newnham et al., 2013; Wood et al., 2017). In glacial periods, continuous forest was predominantly present north of 36°S (Alloway et al., 2007; Newnham et al., 2013). Consequently, pollen records offshore eastern Aotearoa-New Zealand are expected to preserve a vegetation shift from higher proportions of podocarps and hardwoods in interglacials, which are then replaced by beech, small trees and shrubs, and herbs and grasses during glacials. Terrestrial records, such as those from Kaipo Bog (Newnham and Lowe, 2000) or Repongaere Swamp (Wilmshurst et al., 1999), provide valuable insights, but primarily reflect vegetation changes local to those sites and do not extend to the Last Glacial Maximum (LGM; Fig. 1). In contrast, deep-marine records reflect regional vegetation changes, requiring consideration of the long-distance transport mechanisms and potential transport pathways of different pollen types when interpreting past vegetation. For example, many of Aotearoa-New Zealand's native conifers, such as *Prumnopitys* and *Podocarpus* are saccate,[1] making them buoyant and allowing them to be transported long distances in both water and air (Heusser and Balsam, 1977; Holmes, 1990; Tomlinson, 1994; Mildenhall, 2003; Montade et al., 2011; McGann, 2018). The beech pollen taxa *Fuscospora* sp. is not saccate, but despite this demonstrates superior wind transport ability, as evidenced by its high percentages in terrestrial cores from the Chatham Islands, transported over 1000 km from mainland Aotearoa-New Zealand via the dominant westerly winds (Fig. 1; Dodson, 1976; Mildenhall, 1976; Holt et al., 2010). In contrast, many small trees, shrubs, herbs, and grass pollen are either not as robust (thinner walls than robust fern spores like *Cyathea*) or are not as efficient at being transported in wind or water for long distances (Wilmshurst et al., 1999; McGlone, 2001). However, this pattern does not apply to all pollen taxa within these groups, with the shrub *Coprosma*, for example, producing large quantities of well-dispersed pollen that is typically well represented in marine pollen records (Heusser and Van de Geer, 1994; Mildenhall, 2003; Ryan et al., 2012). Despite these differences in pollen transport abilities, studies from Aotearoa-New Zealand comparing terrestrial and marine pollen records have found that the changes in pollen assemblages between glacial and interglacial periods are broadly similar between the onshore and offshore records (Wilmshurst et al., 1999; McGlone, 2001; Ryan et al., 2012). This raises the question of whether this relationship holds true for marine pollen records with greater distances from shore, variable depths, and different sedimentary depositional settings.

[1] Saccate pollen have sacs that are commonly filled with air making them buoyant and 'non-wettable'.

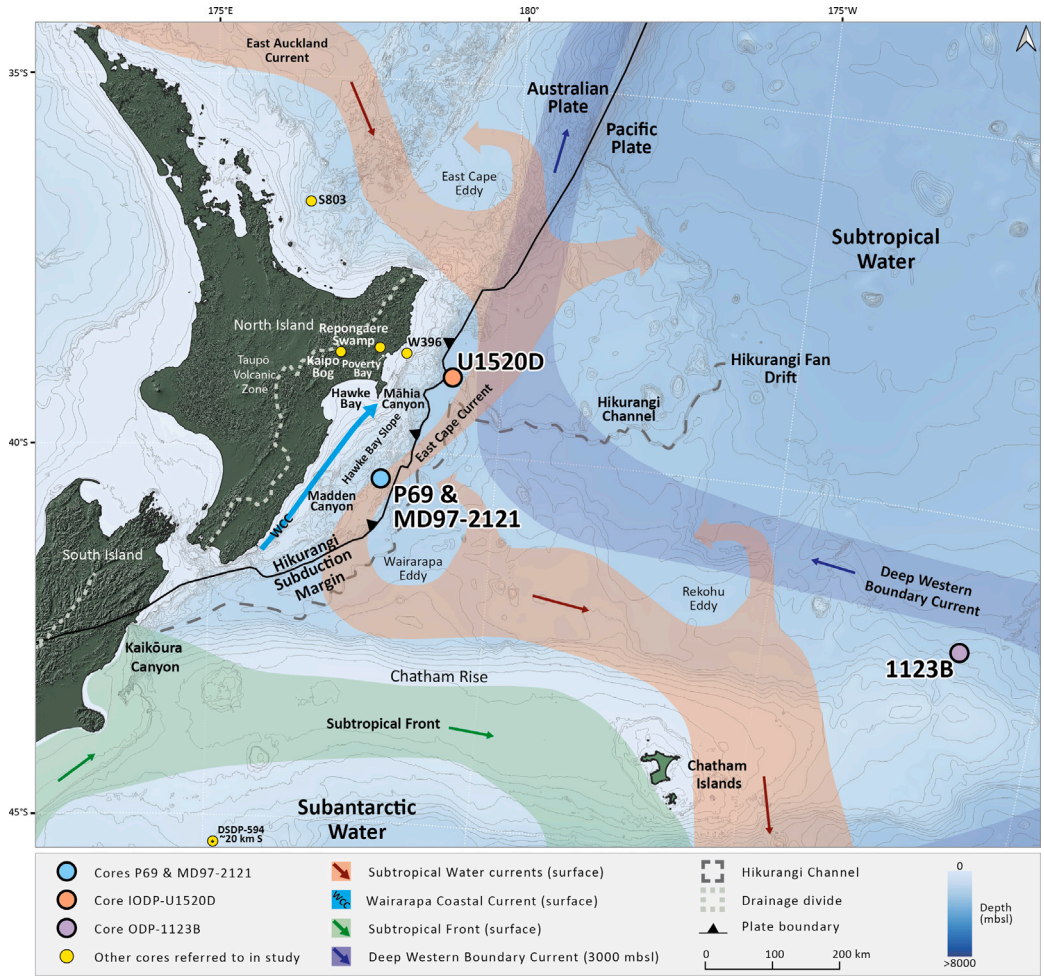

Fig. 1. The east coast of Aotearoa-New Zealand with the locations of sediment cores P69/MD97-2121, IODP-U1520D and ODP-1123B. Shaded areas are surface and deep water ocean currents as in Chiswell et al. (2015).

1.1. Pollen transport pathways to the marine environment in eastern Aotearoa-New Zealand

To explore biases in marine pollen records from eastern Aotearoa-New Zealand, a thorough understanding of the potential pollen transport pathways to the deep ocean is essential. Pollen likely reaches the marine environment through wind (Mildenhall, 1976) or river transport (Mildenhall and Orpin, 2010) and could potentially become trapped in on-land intermediate sedimentary reservoirs (i.e. river banks) during the transport process. As a result of the mountainous landscape formed by the Pacific-Australian tectonic plate boundary, a drainage divide (Fig. 1) exists between the east and west of Aotearoa-New Zealand, with approximately twice as many large rivers flowing to the eastern coast (17 rivers with Strahler Order >6 east of the divide, compared to 9 to the west; Barrell et al., 2013; Abell et al., 2023; National Institute of Water and Atmospheric Research (NIWA), 2025). Many large rivers (Strahler Order ≥7) draining the east coast of the North Island feed into the Hawke's Bay, with the Waiapu and Waipaoa Rivers further north, jointly transporting 35 MT/y of suspended sediment to the coastal zone, accounting for 24% of Aotearoa-New Zealand's total suspended sediment load (Orpin, 2004; Hicks et al., 2011). Additionally, where many of these large rivers meet the ocean, there are estuaries and coastal lagoons (>30 to the east of the North Island divide), which act as effective traps for fine sediment and potentially pollen (Hume and Herdendorf, 1988; Hume et al., 2007; Plew et al., 2018).

Once pollen enters the marine environment, it is likely influenced by both surface (≤200 mbsl), intermediate (200–1200 mbsl) and deep ocean (>2000 mbsl) currents that flow in various directions (Fig. 1). Close to the east coast of the North Island, the surface Wairarapa Coastal Current (WCC) flows northward, and further offshore, the East Cape Current (ECC), transporting Subtropical Water (STW), flows southward (Fig. 1; Chiswell et al., 2015; Stevens et al., 2021). Once the ECC hits the Chatham Rise, it is diverted to the east and forms two large eddies, namely the Wairarapa Eddy and the Rekohu Eddy (Fig. 1; Chiswell, 2005). At intermediate depths, Antarctic Intermediate Water (AAIW) flows in the same direction as the STW surface currents (Bostock et al., 2013; Chiswell et al., 2015). Around 3000 mbsl, the Deep Western Boundary Current (DWBC) flows westward along the northern edge of the Chatham Rise, and then northward along the slope break of northern Aotearoa-New Zealand (Fig. 1; Chiswell et al., 2015). Pollen could be transported and influenced by these ocean currents that flow in all directions at any time in its descent to the seafloor, making it complicated to pinpoint the source of pollen in a marine record (Fig. 1). Once pollen has settled on the seafloor, it can be further reworked and transported by contour currents, forming large sediment drifts including the North Chatham Drift formed by the DWBC (Carter and McCave, 1997; McCave and Carter, 1997; Hall et al., 2002; Bostock et al., 2019) and various drifts along the east coasts continental shelf and slope formed by the ECC and the WCC (Fig. 1; Bailey et al., 2021).

On tectonically active convergent margins, such as the Hikurangi Subduction Margin, another way that pollen can reach the deep ocean is through transport in gravity flows (Talling et al., 2012, 2013, 2022;

Table 1
Sediment core details for P69/MD97-2121, IODP-U1520D, and ODP-1123B, along with the number and depth range of pollen samples used in this study (Stewart and Neall, 1984; Beaufort et al., 1997; Barnes et al., 2019; Saffer et al., 2019).

Sediment core name	Latitude, longitude	Water depth (mbsl)	Core length (m)	Depth range of pollen samples (mbsf)	Number of pollen samples	Pollen data presented in
P69	−40.3833, 177.9967	2195	6.63	0.05–6.45	26	McGlone (2001)
MD97–2121	−40.3822, 177.9947	2314	34.92	25.04–34.9	20	GNS Science (2024) counted by D.C. Mildenhall
IODP-U1520D	−38.9691, 179.1317	3520	515.8	0.74–96.78, 122.04–144.41	36	This paper
ODP-1123B	−41.7860, −171.4990	3290	488.66	1–8.9	7	Mildenhall et al. (2004)

McDonald et al., 2024). The Hikurangi Margin (Lewis and Pettinga, 1993; Wallace et al., 2009) runs along the east coast of northern Aotearoa-New Zealand and consists of a network of canyons that incise the continental shelf, including the Kaikōura Canyon (Lewis and Barnes, 1999; Mountjoy et al., 2018) and the Māhia Canyon (Fig. 1; Pedley et al., 2010; Shorrock et al., 2025). Sediment is transported in these canyons via gravity flows including turbidity currents, debris flows, and landslides which can be triggered by numerous mechanisms including tectonic events such as earthquake shaking (Piper and Normark, 2009; Pouderoux et al., 2012b; Mountjoy et al., 2018; Howarth et al., 2021), or storm events (Piper and Normark, 2009; Pouderoux et al., 2012a; Clare et al., 2016). When turbidity currents exit the canyons, they can continue to debouch into deep water channels, including the Hikurangi Channel, until they lose momentum and deposit their sediment either within the channel or on the overbank lateral to the channel via overspill (Fig. 1; Lewis and Pantin, 2002; Tek et al., 2022; Shorrock et al., 2025). McDonald et al. (2024) found that in recent (<150 years) Hikurangi Margin turbidites, pollen and spores reached concentrations as high as 10,000 grains/g, showing that significant amounts of pollen are transported to the deep ocean by turbidity currents along active margins to distances of at least 670 km down axial channels like the Hikurangi Channel.

2. Methodology

2.1. P69/MD97-2121

The P69/MD97-2121 record combines pollen records from two adjacent sediment cores: P69 (McGlone, 2001) and MD97-2121 (GNS Science, 2024; Figs. 1 and 2; Table 1). We combine these pollen records due to the proximity of the core sites (~200 m apart) and because core MD97-2121 extends the P69 record (Figs. 1 and 2; Table 1). The core sites for P69 and MD97-2121 are located ~100 km southeast of the Wairarapa Coast and were retrieved from 2195 and 2314 mbsl, respectively (Figs. 1 and 2; Table 1). The cores are positioned within a Hawke Bay slope basin, where initial core logging found no evidence of turbidites and the sediment was interpreted to be hemipelagic (Figs. 1 and 2; Stewart and Neall, 1984; Carter and Manighetti, 2006). Core P69 is 6.45 m long and is composed of silt and clay, with laminae of silty-sandy reworked tephra from the Taupō Volcanic Zone (Figs. 1 and 2; Stewart and Neall, 1984; Nelson et al., 2000; McGlone, 2001). Following the age model used in McGlone (2001), the P69 record extends to the MIS2 glacial at 25.6 ka (Fig. 2; Table 1; Stewart and Neall, 1984). The pollen record for the P69 sediment core (McGlone, 2001) is comprised of 26 samples which cover the entire length of the core (Table 1).

Core MD97-2121 (Beaufort et al., 1997) is 34.92 m long and consists of similar lithofacies types as P69, which was originally interpreted as hemipelagites and reworked tephras (Fig. 2; Carter et al., 2002; Carter and Manighetti, 2006; Alloway et al., 2007). The base of MD97-2121 is dated at 135 ka, near the end of the glacial MIS6 (Fig. 2; Carter and Manighetti, 2006; Pahnke and Sachs, 2006; Anderson et al., 2020). The MD97-2121 pollen record is comprised of 20 pollen samples from the lower 9.8 m of the core, with unpublished raw pollen counts retrieved from the Institute of Geological and Nuclear Sciences (GNS Science) Fossil Record Electronic Database (FRED; Table 1; GNS Science, 2024).

2.2. IODP-U1520D

IODP sediment core U1520D, was retrieved from 3520 mbsl (Figs. 1 and 2; Table 1; Barnes et al., 2019; Saffer et al., 2019) from the Hikurangi Trough, ~110 km southeast of the Poverty Bay coast (Figs. 1 and 2). We focus on the upper 189 m of the core, which consists of a sequence of mostly silt-rich turbidites (Fig. 2; Table 1; Barnes et al., 2019; Saffer et al., 2019; Woodhouse et al., 2024). Woodhouse et al. (2024) created an age model for the upper 110 m of the core, finding that MIS1 is ~10 m thick and MIS2 is ~85 m thick (Fig. 2). They attributed the higher sedimentation in MIS2 to the lower sea level which was ~134 m below present at the LGM, resulting in the Māhia Canyon directly tapping nearshore sediment transport systems (Fig. 1; Woodhouse et al., 2024). Seismic reflection data indicates that the section of IODP-U1520D from 189-110 m is likely a distal part of the Ruatōria Mass Transport Deposit (RMTD; Lewis et al., 1998; Collot et al., 2001; Barnes et al., 2019; Gamboa et al., 2019; Saffer et al., 2019; Crundwell and Woodhouse, 2024a). Shipboard observations noted that IODP-U1520D lacks clear evidence of soft-sediment deformation in the beds (Barnes et al., 2019), leading to the interpretation that this section of IODP-U1520D represents an intact block of the RMTD (Gamboa et al., 2019).

To further improve and extend the age control in IODP-U1520D, we used radiocarbon (Woodhouse et al., 2024), foraminifera assemblages (Crundwell and Woodhouse, 2024a,b), stable isotopes (this study, Noda et al. 2024, Woodhouse et al. 2024) and tephra (Clarke, 2023; Pank et al., 2025) stratigraphic markers to develop a new age model using the BIGMACS software (Fig. 3; Table A.3; Lee et al., 2023). BIGMACS creates a Bayesian age model that, along with radiocarbon (Heaton et al., 2020) and other age tie points, incorporates $\delta^{18}O$ measurements and aligns them to global benthic stacks (Lee et al., 2023). To supplement the IODP-U1520D $\delta^{18}O$ record by Noda et al. (2024) and Woodhouse et al. (2024), 15 additional samples of the benthic foraminifera species *Uvigerina peregrina* were selected for stable isotope analyses and were run in the Stable Isotope Laboratory at the Centre for Geoanalytical Mass Spectrometry at the University of Queensland on the Isoprime Dual Inlet Mass Spectrometer. The combined 87 $\delta^{18}O$ measurements were entered into BIGMACS and aligned with the LR04 Benthic Stack (Table A.3; Lisiecki and Raymo, 2005; Lee et al., 2023).

Using the new age model for IODP-U1520D, 36 pollen samples were selected to target the MIS6-5e (130 ka) and MIS2-1 (14 ka) glacial–interglacial transitions, allowing comparison of pollen assemblage changes over the last glacial cycle with the existing P69/MD97-2121 and ODP-1123B pollen records (Table 1). As IODP-U1520D is dominated by turbidites (Woodhouse et al., 2024), all pollen samples were sampled from the upper silt-clay-rich parts of the turbidites for optimal pollen recovery (McDonald et al., 2024). *Lycopodium clavatum* tablets (Stockmarr, 1971) were added as a pollen-counting standard to allow for the calculation of pollen concentrations. Conventional pollen extraction methods (Faegri et al., 1989) were followed, including reacting with 10% hydrochloric acid to remove carbonates, removing humic acid with a 1:1 ratio of potassium hydroxide and sodium pyrophosphate, sieving through an 11 μm mesh, separating the organics from the bulk material with sodium polytungstate (specific

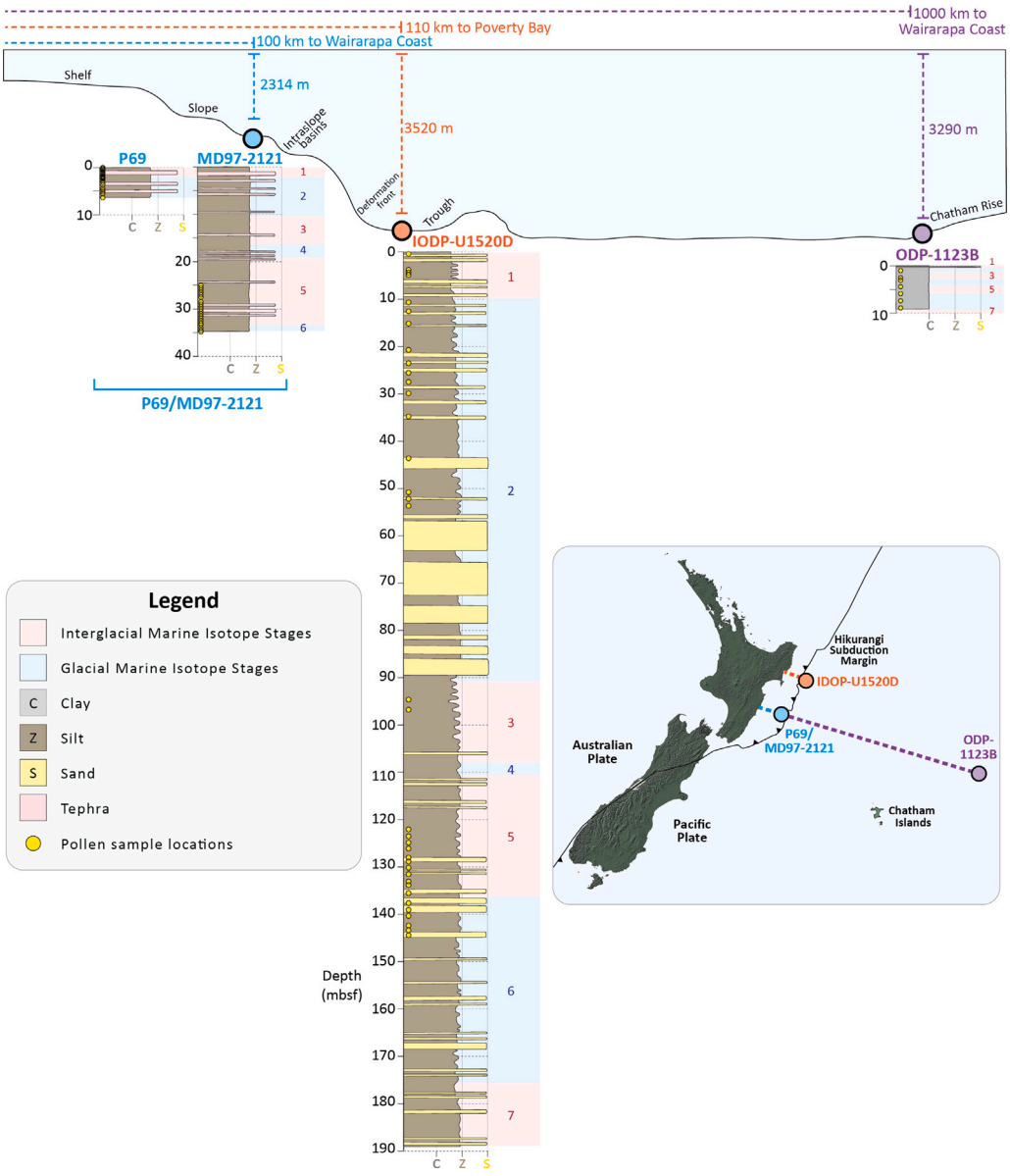

Fig. 2. Stylised sediment logs of cores P69, MD97-2121, IODP-U1520D and ODP-1123B. The cross-section shows the depositional environments of each core, the distances from the coast, and the depths below the sea level.

gravity=2 g/cm^3; Campbell et al., 2016; van den Bos et al., 2020), acetolysis (9:2 mixture of acetic anhydrite and concentrated sulphuric acid), alcohol dehydration (tertiary butyl alcohol), and mounting in silicon oil. Pollen grains were identified using key texts (Pocknall, 1981a,b,c; Large and Braggins, 1991; Moar et al., 1993) and counted using PolyCounter (Nakagawa, 2007). Where possible, >250 dryland pollen grains were counted for each sample. Here we present the pollen record for IODP-U1520D for the first time.

2.3. ODP-1123B

ODP core 1123B, collected from 3290 mbsl, is the distal-most core studied here, located >1000 km offshore Aotearoa-New Zealand on the northern flank of the Chatham Rise (Figs. 1 and 2; Table 1; Carter et al., 1999). This study focuses on the upper 8.7 m of ODP-1123B, which extends back to 190 ka near the end of MIS7 (Mildenhall et al., 2004). Sediment at the site is interpreted to be from both terrigenous and biogenic–pelagic sources that are reworked into contourite drifts by the flow of the DWBC (Fig. 1; Hall et al., 2001, 2002; Weedon and Hall, 2004). As a result, the sediment from the last 190 ka in ODP-1123B is dominated by clay-rich nannofossil oozes (Fig. 2; Carter et al., 1999; Mildenhall et al., 2004). The pollen record from ODP-1123B is published in Mildenhall et al. (2004), with the raw pollen counts used in this study retrieved from FRED (GNS Science, 2024). This ODP-1123B record extends to the early Pliocene, however, we only use the 7 samples from the upper 8.9 m of the core in this study, covering the last glacial cycle back to the start of MIS6 (Table 1; Carter et al., 1999; Mildenhall et al., 2004).

2.4. Data analysis and statistics of all three pollen records

For all three records, we split pollen taxa into the following groups: podocarps and hardwoods, beech, small trees and shrubs, herbs and grasses, and unidentified pollen. Unidentified pollen were grains that were damaged and too difficult to confidently identify. The pollen groups were then used to calculate the overall pollen percentages, which were plotted in Tilia (Grimm, 2020). We include unidentified pollen because they are a part of the dryland pollen and if they were

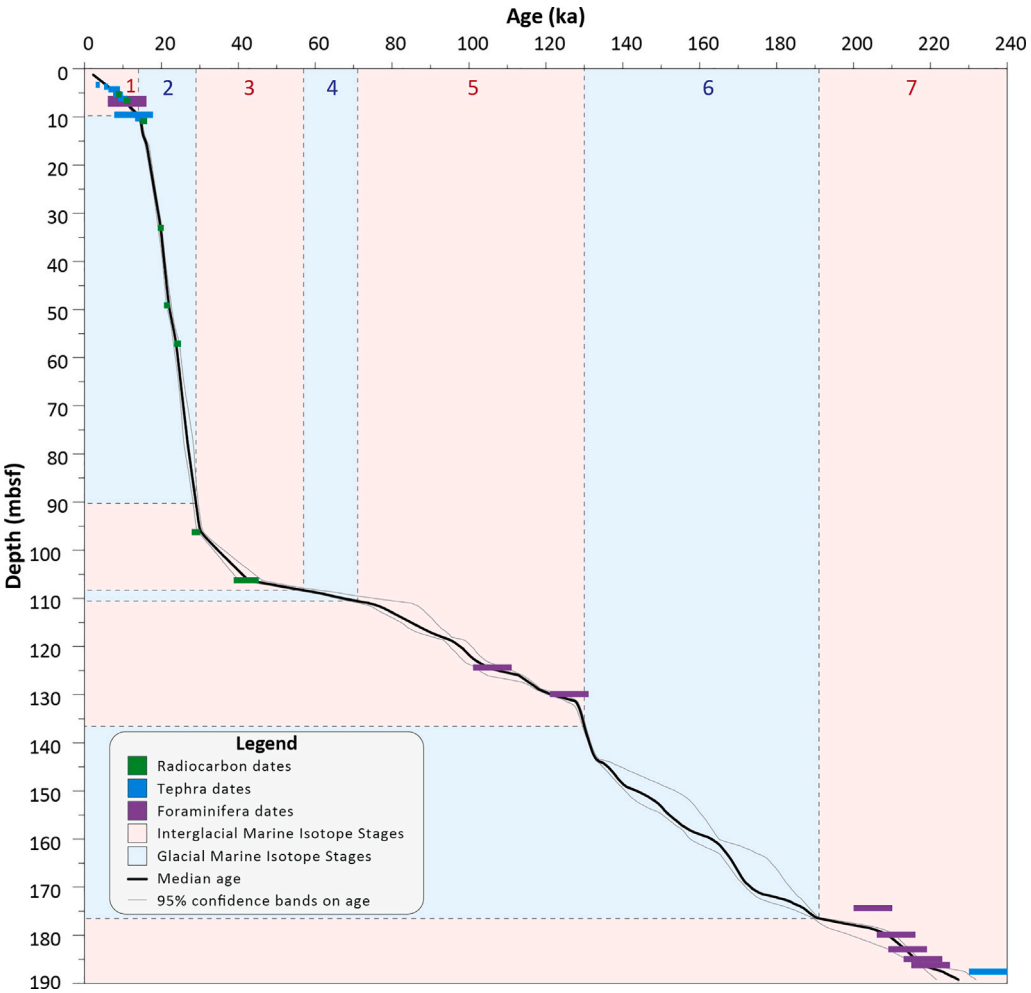

Fig. 3. Age model for the upper 190 m of sediment core IODP-U1520D. The width of the green (radiocarbon), blue (tephra) and purple (foraminifera) coloured bars represents the error on each age marker.

removed, other pollen groups would become exaggerated, which is particularly important in P69 where one sample has 29% unidentified pollen. Spores from ferns and fern allies were excluded from the overall pollen percentage calculations as spores are typically not included in palynological studies in Aotearoa-New Zealand as they dilute the signal from other pollen taxa (Newnham et al., 2007a; Augustinus et al., 2011). To explore differences in variance between glacial and interglacial pollen assemblages, Principal Component Analysis (PCA) was conducted in PAST (Hammer and Harper, 2001), using the podocarps and hardwoods, beech, small trees and shrubs, and herbs and grasses pollen group percentages from all samples across the three core sites. For the PCA, we removed unidentified pollen because this group was not represented across all three records and skewed the PCA bi-plots.

Sediment Accumulation Rates (SAR) for MIS 1, 2, 5, and 6 were calculated by dividing the sediment accumulated by the duration of each Marine Isotope Stage. We compared the SAR for each MIS to the average pollen and spore concentrations from the P69/MD97-2121 and IODP-U1520D records, using the methods of Stockmarr (1971) to calculate concentrations. While the same marker spores and equations were utilised for calculating pollen and spore concentrations in both records, it is important to note that the P69/MD97-2121 record used dry sediment samples, in contrast to the IODP-U1520D record, which used wet sediment samples. Consequently, the weights applied for calculating concentrations in the IODP-U1520D record would have been greater, meaning that the pollen and spore concentrations for the IODP-U1520D record will be lower than those from the P69/MD97-2121 record. Pollen and spore concentrations were unavailable for ODP-1123B, as Mildenhall (2003) indicated that the pollen recovery was too sparse to calculate concentrations.

3. Results

3.1. P69/MD97-2121

The P69/MD97-2121 record shows variability in pollen assemblages between interglacial and glacial periods (Fig. 4). Podocarps and hardwoods constitute the dominant group in P69/MD97-2121, while other pollen groups are less abundant (Fig. 4). The pollen record begins near the end of MIS6 (~135 ka), where podocarps and hardwoods constitute almost half the pollen (49%), and beech (17%), small trees and shrubs (23%), and herbs and grasses (11%) are present in lesser percentages (Fig. 4). A notable shift in the pollen assemblage occurs during the transition to MIS5e (130 ka), with podocarps and hardwoods increasing to a maximum of 97% at 124 ka (an increase of 48%), while all other groups subsequently decline (Fig. 4). When the P69 record begins in MIS2 (25.6 ka), podocarps and hardwoods are as low as 37%, and other pollen groups are higher, with beech (18%) being the most dominant among these (Fig. 4). A glacial peak in podocarps and hardwoods occurs around 22 ka (63%), but the group subsequently declines to the lowest percentage of the entire record (27%) by 17 ka (Fig. 4).

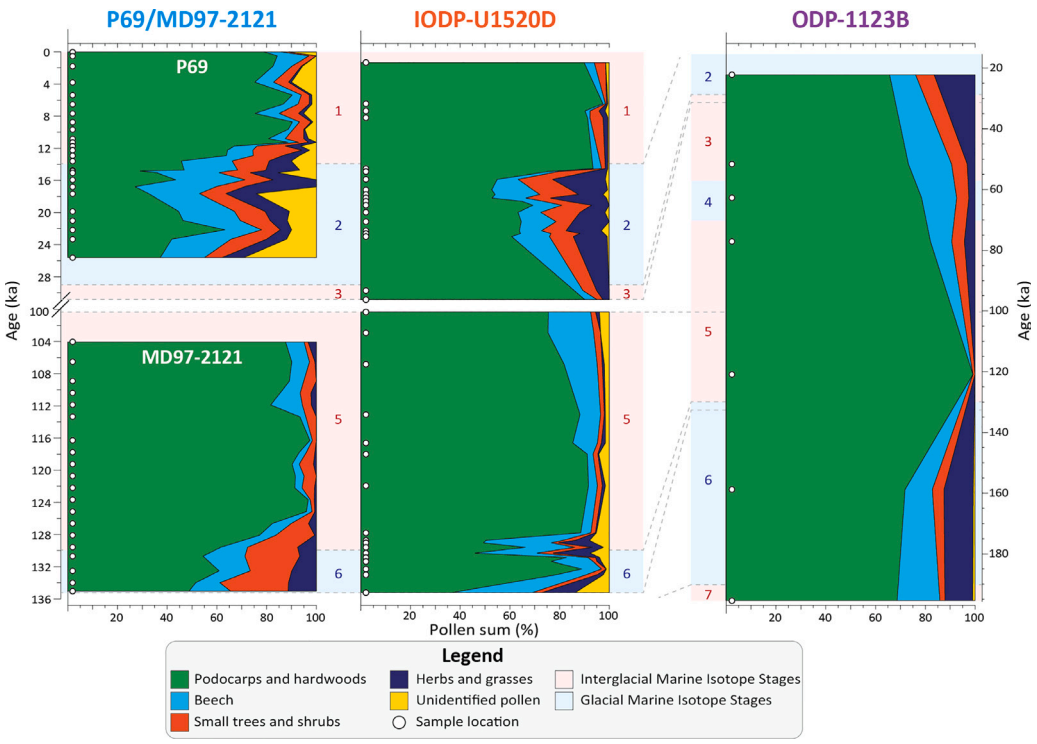

Fig. 4. Pollen percentage plots for the cores P69/MD97-2121, IODP-U1520D and ODP-1123B. Note that P69/MD97-2121 and IODP-U1520D are on the same age scale (with a time break from 100-31 ka), and ODP-1123B is on a different and continuous age scale, with dashed lines showing the time intersections of the pollen records.

Table 2
Average percentages of different pollen taxa groups in glacial and interglacial periods in the cores P69/MD97-2121, IODP-U1520D and ODP-1123B.

Pollen taxa group	P69/MD97-2121	IODP-U1520D	ODP-1123B
Interglacial pollen average percentage			
Podocarps and hardwoods	83%	82%	81%
Beech	7%	10%	11%
Small trees and shrubs	6%	3%	4%
Herbs and grasses	2%	3%	5%
Glacial pollen average percentage			
Podocarps and hardwoods	44%	66%	72%
Beech	21%	13%	12%
Small trees and shrubs	14%	9%	6%
Herbs and grasses	11%	10%	10%

Beech pollen reaches a maximum of 36% at 15 ka, while podocarps and hardwoods are still low (29%), and small trees and shrubs are 14% and herbs and grasses are 12% (Fig. 4). During the deglacial transition from MIS2 to MIS1, podocarps and hardwoods increase again, remaining between 75%–90% after 11 ka, and all other taxa groups decrease (Fig. 4). Unidentified pollen is particularly high in MIS2 and MIS1, with a maximum of 29% at 25.6 ka (Fig. 4). PCA results show that interglacial samples from P69/MD97-2121 plot strongly around the podocarps and hardwoods loading vector (Fig. 5). In contrast, the glacial samples from P69/MD97-2121 show higher spread on the PCA bi-plot, with all samples plotting in the negative PC1, which is in the opposite direction of the podocarps and hardwoods loading vector in the positive PC1 (Fig. 5).

The shifts between glacial and interglacial pollen assemblages occur despite no clear changes in the sediment, which remains consistently a clayey-medium-silt, interspersed with occasional reworked tephra horizons (Fig. 2). In addition, SAR vary through the record, with higher rates during glacial periods (MIS6=0.34 m/ka, MIS2=0.58 m/ka) compared to interglacial periods (MIS5=0.24 m/ka, MIS1=0.16 m/ka; Fig. 6). An inverse trend is shown in the pollen and spore concentrations, which are generally higher in the interglacials (MIS5=17674 grains/g, MIS1=20331 grains/g) and lower in the glacials (MIS 6=8390 grains/g, MIS2=9851 grains/g; Fig. 6).

3.2. IODP-U1520D

The new age model for IODP-U1520D extends to 227 ka (MIS7) at 189 mbsf (Fig. 3) and the pollen record covers the transition from MIS6-5e (135-100 ka) and from the end of MIS3 (31 ka) to the top of MIS1 (Fig. 4). Overall, podocarps and hardwoods are the dominant group in IODP-U1520D, with other taxa groups being less abundant (Fig. 4). At 135 ka podocarps and hardwoods are low at 37%, then sharply increase to a maximum of 89% at 132 ka (Fig. 4). At the beginning of MIS5e (130 ka) podocarps and hardwoods decrease to 46%, while beech rises to 25% (Fig. 4). Following this, podocarps and hardwoods increase again to 92% at 122 ka, gradually decreasing for the remainder of the MIS5 record (Fig. 4). At the end of MIS3

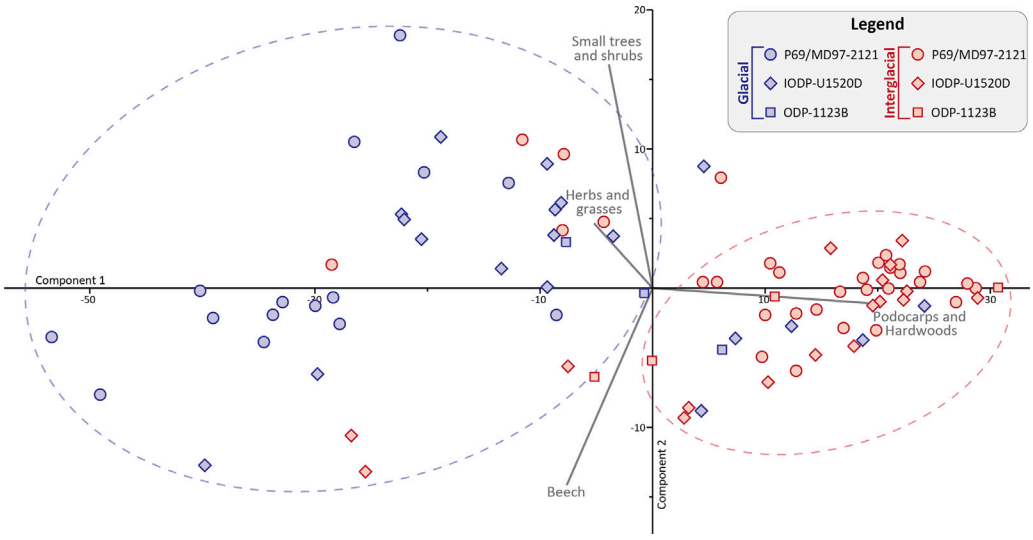

Fig. 5. Principal Component Analysis bi-plot illustrating the variance in glacial and interglacial pollen samples from the P69/MD97-2121, IODP-U1520D, and ODP-1123B records.

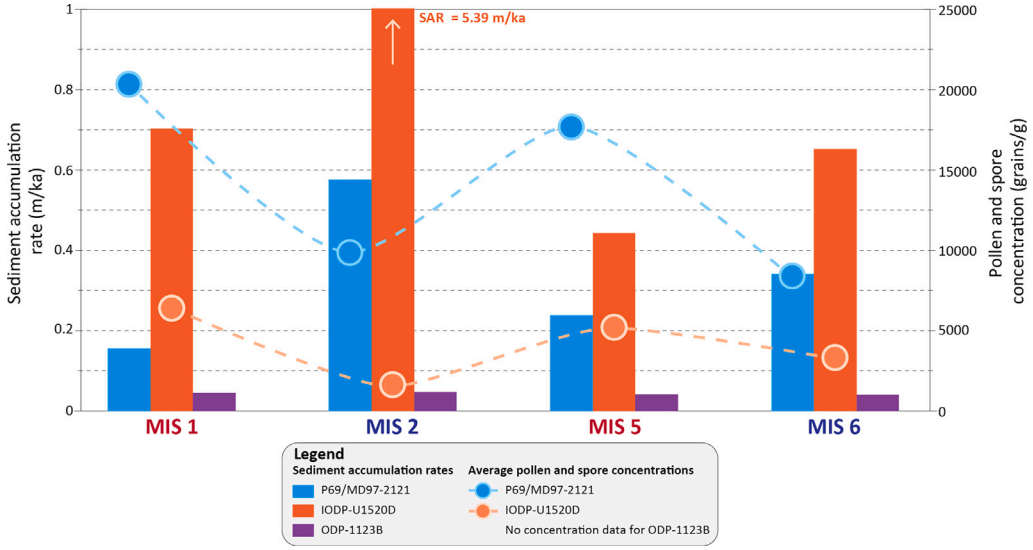

Fig. 6. Sediment accumulation rates and pollen and spore concentrations from the P69/MD97-2121, IODP-U1520D and ODP-1123B records in glacial (MIS6&2) and interglacial (MIS5&1) periods. Note there is no pollen and spore concentration data for the ODP-1123B record (Mildenhall, 2003).

(31 ka), podocarps and hardwoods are a high 90% (Fig. 4). In MIS2, podocarps and hardwoods drop as low as 53% at 17 ka, with beech (17%), small trees and shrubs (15%), and herbs and grasses (15%) increasing (Fig. 4). At the transition from MIS2 to MIS1, podocarps and hardwoods rise again, peaking at 98% at 6 ka, while the other pollen groups decline (Fig. 4). In the PCA bi-plot, interglacial samples from IODP-U1520D plot strongly around the podocarps and hardwoods loading vector, whereas glacial samples are more variable, with most glacial samples plotting near the small trees and shrubs and herbs and grasses loading vectors (Fig. 5).

The age model (Fig. 3) shows that the sedimentation rate changed significantly across the Marine Isotope Stages. In MIS6 the SAR is 0.65 m/ka, decreasing to 0.44 m/ka in the interglacial MIS5 (Fig. 6). Through these intervals the sediment is mostly turbidites, with potential contourite sediments (Barnes et al., 2019). MIS2 has the highest SAR of 5.39 m/ka, with some of the turbidites becoming thicker and coarser grained (Figs. 2 and 6; Woodhouse et al., 2024). The SAR drops in the MIS1 interglacial to 0.70 m/ka, with similar sedimentary facies as MIS5 and MIS6 (Figs. 2 and 6; Woodhouse et al., 2024). Average pollen and spore concentrations in IODP-U1520D are higher during interglacials (MIS5=5203 grains/g, MIS1=6392 grains/g) compared to glacials (MIS6=3319 grains/g, MIS2=1628 grains/g), corresponding with the lower SAR in the interglacials (Fig. 6).

3.3. ODP-1123B

The ODP-1123B record shows broad differences between glacial and interglacial pollen assemblages (Figs. 2 and 4). Near the MIS7-6 transition (195 ka), podocarps and hardwoods are relatively low at 69%, while beech and herbs and grasses make up 17% and 11% of the record, respectively, with much lower percentages of small

trees and shrubs (2%; Fig. 4). In the single sample from MIS5 (121 ka), podocarps and hardwoods are 99%, with all other groups either absent or comprising less than 0.9% (Fig. 4). Following this MIS5 peak, podocarps and hardwoods decline for the remainder of the record, dropping as low as 66% in MIS2 (22 ka), which corresponds with an increase in beech (10%), small trees and shrubs (8%), and herbs and grasses (16%; Fig. 4). The pollen samples from ODP-1123B do not show much variability in the PCA bi-plot, with most of the samples grouping around the centre of the four loading vectors of podocarps and hardwoods, beech, small trees and shrubs, and herbs and grasses (Fig. 5).

The sediment in ODP-1123B is a clayey nannofossil ooze and shows slight colour changes, from greenish-grey during glacial periods (approximately 50% $CaCO^3$) to whiter in interglacial periods (approximately 80% $CaCO^3$; Mildenhall et al., 2004). These changes are attributed to higher terrigenous flux to the site during glacial periods (Mildenhall et al., 2004). The SAR remains consistently low (approximately 0.04 m/ka) at ODP-1123B, with the most variability between Marine Isotope Stages being 0.0074 m/yr (Fig. 6). Pollen concentration was not calculated for ODP-1123B, as Mildenhall (2003) noted that the pollen was too sparse and it was not feasible to add a pollen spike to calculate pollen concentration (Fig. 6).

4. Discussion

The pollen assemblages from the P69/MD97-2121, IODP-U1520D, and ODP-1123B records show variability between glacial and interglacial periods (Figs. 4 and 5). Generally, podocarps and hardwoods are more abundant in interglacials, with average percentages of 83%, 82% and 81% in the P69/MD97-2121, IODP-U1520D, and ODP-1123B records, respectively (Fig. 4; Table 2). This is also evident in the PCA bi-plot of all samples, where the majority of pollen samples from interglacials group around the podocarps and hardwoods vector (Fig. 5; Table 2). Conversely, in glacial periods, podocarps and hardwoods are lower, with average percentages of 44%, 66%, and 72% in the P69/MD97-2121, IODP-U1520D, and ODP-1123B records, respectively (Fig. 4). In glacial periods, the decline in podocarps and hardwoods is substituted by an increase in the groups beech, small trees and shrubs, and herbs and grasses (Fig. 4). This is supported by the PCA bi-plot, as in contrast to samples from interglacial periods, which are grouped strongly around podocarps and hardwoods, pollen samples from glacial periods are more spread out, grouping broadly around the vectors for beech, small trees and shrubs, and herbs and grasses (Fig. 5). P69/MD97-2121 shows larger swings between glacial and interglacial pollen assemblages, whereas the changes in IODP-U1520D and ODP-1123B are more subdued (Fig. 4).

4.1. Pollen source and transport mechanisms to deep-marine sites

The overall similarity in pollen records between the three cores, despite slight variations in glacial periods, is surprising given the different locations, depths, and potential mechanisms of sediment and pollen transport to these sites (Figs. 1, 2 and 4). Sediment and pollen likely follow a more direct transport pathway to P69/MD97-2121 than to the other two sites, as it is the shallowest and most proximal to land (Figs. 1 and 2; Table 1). Previous studies by Nelson et al. (2000) and Carter and Manighetti (2006) interpreted the clayey-medium-silt sediment in P69/MD97-2121 to be hemipelagic with no visual evidence of turbidites. However, Camp's (2020) benthic foraminiferal provenance and detailed computed tomography sedimentological facies analyses of Holocene-aged cores from the same and nearby semi-confined basins on the Hawke Bay Slope, instead interpreted deposition by silt-dominated sediment gravity flow processes (Fig. 1; McArthur et al., 2022). Nelson et al. (2000) and Carter and Manighetti (2006) interpreted "reworked tephra" in P69/MD97-2121, showing recognition of sediment reworking. This suggests that the pollen transport pathway to P69/MD97-2121 is more complicated than previously interpreted and that there is probably a mix of transport processes impacting the site, including ocean currents, sediment gravity flows, and reworking by bottom currents. Multiple stages of reworking may explain the high proportion of unidentified pollen in MIS2 and MIS1 in P69/MD97-2121, although it is also likely influenced by differences in counting and categorisation methods used by the palynologist who analysed these samples compared to those for IODP-U1520D and ODP-1123B (Table 1). Adding to the complexity of pollen transport to this site, McGlone (2001) noted the similarity between the interglacial pollen assemblages in P69 and marine core S803 from the Bay of Plenty (Wright et al., 1995), and interpreted this as evidence that pollen is likely transported from more northern sources to P69 via the southward-flowing ECC (Fig. 1). P69/MD97-2121 has the highest pollen and spore concentration of the three cores, which is likely also a product of the sites' proximity to land and relatively direct transport pathway for pollen (Figs. 1 and 6). In glacial periods P69/MD97-2121 has higher average percentages of beech (21%), small trees and shrubs (14%), and herbs and grasses (11%) than in IODP-U1520D and ODP-1123B (Fig. 4; Table 2). This is likely due to P69/MD97-2121 being closer to the hinterland pollen source and located at a shallower depth compared to IODP-U1520D and ODP-1123B, making it more likely to receive pollen types that are less efficiently transported over long distances (e.g., non-saccate pollen) than the more distal sites.

Sediment and pollen were primarily transported to IODP-U1520D by turbidity currents, as evidenced by the multiple turbidites throughout the record (Fig. 2; Woodhouse et al., 2024; Shorrock et al., 2025). The sediment and pollen in IODP-U1520D are interpreted to be sourced from the shelf and canyons offshore the east coast of Aotearoa-New Zealand, with the mouth of the nearby transverse Māhia Canyon located approximately ~50 km southwest of the core site (Fig. 1; Lunenburg, 2017; Woodhouse et al., 2024; Shorrock et al., 2025). While most sediment delivered to IODP-U1520D likely originates from the Māhia Canyon, some turbidites may be sourced from canyons further south along the Hikurangi Margin, as turbidity currents can travel long distances (Talling et al., 2022; Maier et al., 2024), especially in well-developed channels like the Hikurangi Channel (Fig. 1; Lewis, 1994; Lewis et al., 1998). For example, Maier et al. (2024) found a 2 cm thick turbidite in the Hikurangi Fan Drift (Lewis et al., 1998) ~1300 km down flow from the Kaikōura Canyon which was a result of a turbidity current triggered by the 2016 Kaikōura Earthquake (Clark et al., 2017; Hamling et al., 2017; Litchfield et al., 2018; Mountjoy et al., 2018; Howarth et al., 2021; McDonald et al., 2024). Shorrock et al. (2025) show that during the last 42 ka the contribution of sediment to site IODP-U1520D was mostly from transverse sediment delivery from the Māhia Canyon, with less sediment contribution from the axial Hikurangi Channel (Fig. 1; Noda et al., 2024; Woodhouse et al., 2024). Therefore, it is likely that most of the sediment and pollen that is delivered to IODP-U1520D by turbidity currents is sourced from shallower sediments on the shelf near the head of the Māhia Canyon (Lunenburg, 2017; Woodhouse et al., 2024; Shorrock et al., 2025). Although Shorrock et al. (2025) found the contribution from the Hikurangi Channel to be minor, turbidites from a southern source could still affect the final pollen record and interpretations of past vegetation, highlighting the importance of understanding both transverse and axial sediment transport contributions. In the shallow marine core W396 (63 mbsl) from the Hawke Bay shelf, Wilmshurst et al. (1999) found a high level of the extinct beech pollen *Brassospora*, interpreted to have originated from Tertiary sedimentary rocks in the Waipaoa River catchment (Fig. 1), as was also noted in P69 in McGlone (2001). Therefore, the presence of *Brassospora* in IODP-U1520D (see supplementary data) provides additional evidence for the dominance of a North Island pollen source to the site. Therefore, the overall similarity in pollen assemblages between IODP-U1520D and P69/MD97-2121 could be attributed to their shared North Island pollen source, despite having different sediment accumulation rates and sedimentary characteristics (Figs. 2

and 6). McDonald et al. (2024) suggested that turbidite-dominated records can produce vegetation reconstructions similar to those of other marine pollen records, with similar pollen assemblages between the turbidite-dominated IODP-U1520D record and the P69/MD97-2121 record supporting this (Fig. 4).

The primary difference between IODP-U1520D and P69/MD97-2121 occurs during MIS6, where IODP-U1520D shows a distinct spike in podocarps and hardwoods, interpreted as marking the start of the interglacial MIS5e (Fig. 4). However, this spike is followed by a return to glacial-like levels of podocarps and hardwoods and an increase in beech pollen (Fig. 4). As this trend is not seen in the P69/MD97-2121 record, another mechanism or process is likely influencing the IODP-U1520D record in this interval. Interestingly, in the IODP-U1520D interval where beech pollen increases, the pattern is mirrored by an increase in $\delta^{18}O$ from benthic foraminifera (see supplementary Fig. B.8). We hypothesise that the shift in both pollen and $\delta^{18}O$ could be due to either 1. A repeating sedimentary sequence resulting from deformation from the RMTD or 2. Reworking of glacial sediment and pollen. The glacial-like pollen and $\delta^{18}O$ signal is from a total of four turbidite samples from 137.6-133 mbsf and in this interval there are a total of 24 turbidite beds. This interval is within the interpreted RTMD (189-110 m) so it is possible that the glacial-like pollen and $\delta^{18}O$ signal is due to a repeating stacked sedimentary sequence from deformation by the RMTD (Collot et al., 2001; Gamboa et al., 2019). During mass transport events, sediment may undergo deformation processes such as folding and thrust faulting, potentially leading to the repetition of sedimentary sequences, making this hypothesis plausible (Fig. B.8; Bull et al., 2019; Cardona et al., 2020; Alsop et al., 2024). However, the four turbidites sampled may have been reworked from older glacial sediments, and to test whether this or a repeating sequence from the RMTD is responsible, more pollen samples are needed to see if the glacial-like pollen and $\delta^{18}O$ signal appear in other turbidite beds. Additionally, detailed sedimentary analysis of this interval to identify and assess sedimentary features related to Mass Transport Deposit deformation would be beneficial.

The transport pathway for pollen to reach site ODP-1123B is complex as this site is 900 km further from Aotearoa-New Zealand than P69/MD97-2121, and sits in ~1000 m deeper water (Figs. 1 and 2). The distance from Aotearoa-New Zealand is reflected in ODP-1123B having the lowest pollen recovery of the three cores (see Section 2), with some samples devoid of pollen (Fig. 6; Mildenhall, 2003). The very low SAR at ODP-1123B, along with the mostly biogenic–pelagic sedimentation, shows that very little terrigenous material, including pollen, is reaching this distal site (Figs. 1, 2 and 6). Podocarps and hardwoods are abundant in ODP-1123B, only dropping as low as 66% in MIS2, compared to minimums of 27% in P69/MD97-2121 and 37% in IODP-U1520D (Fig. 4). Mildenhall (2003) attributed the high percentages of podocarp pollen in ODP-1123B to the saccate morphology of most podocarps (i.e. *Prumnopitys* and *Podocarpus*), giving them the ability to float long distances compared to other pollen types. This was also found by Crouch et al. (2010), who noted that saccate conifer pollen occurred in the highest percentages (compared to other surface samples from offshore eastern Aotearoa-New Zealand) along the northern flank of the Chatham Rise, underlying the easterly flowing Subtropical Front (Fig. 1). Crouch et al. (2010) also noted that in all 38 surface samples (latitudes from 33-54°S), beech (<4% *Fuscospora* sp.) and angiosperm pollen (<10%) were low. They attributed this to these taxa not being transported as efficiently in water and instead falling out sooner than saccate pollen types, which may explain the low percentages of beech, small trees and shrubs, and herb and grass pollen in ODP-1123B, compared to P69/MD97-2121 and IODP-U1520D (Table 2). Terrestrial sediment cores from the Chatham Islands (~500 km southwest of ODP-1123B) contained up to 26% wind-blown pollen from Aotearoa-New Zealand, with some of this exotic pollen entirely consisting of *Fuscospora* sp., demonstrating the long-distance wind transport capability of beech pollen (up to 725 km; Fig. 1; Mildenhall, 2003). Therefore, pollen reaching site ODP-1123B is likely from a mix of both wind and ocean current transport. As well as being more distal than P69/MD97-2121 and IODP-U1520D, ODP-1123B also lies directly under the northward-flowing DWBC, meaning that it could be receiving pollen transported from further south (Fig. 1; Chiswell et al., 2015). If pollen was sourced from further south in Aotearoa-New Zealand, the record would likely show higher beech pollen percentages and lower podocarp pollen percentages, similar to deep-marine core DSDP-594, which contained up to 80% beech pollen and generally <20% *Prumnopitys+Podocarpus* pollen (Figs. 1 and 4; Heusser and Van de Geer, 1994). However the dominance of podocarps and hardwoods in ODP-1123B (average of 77%) makes it more comparable to P69/MD97-2121 and IODP-U1520D with average podocarps and hardwood percentages of 70% and 73%, respectively, meaning that ODP-1123B likely has a North Island pollen source (Fig. 4; Mildenhall, 2003).

4.2. Sediment accumulation rates and pollen concentration

The SAR in IODP-U1520D is the highest of the three cores, particularly during the MIS2 glacial, and the pollen and spore concentration is lower than in P69/MD97-2121 (Fig. 6). Thus, at site IODP-U1520D, the exceptionally high SAR and turbidite recurrence intervals (see Woodhouse et al., 2024) likely diluted the pollen and spores (Fig. 6). In both P69/MD97-2121 and IODP-U1520D, the pollen concentration is higher when the SAR is lower in interglacial periods (i.e. MIS5&1 in Fig. 6). High pollen concentration in interglacials could reflect the higher pollen output from podocarp taxa, which had greater coverage in the North Island during interglacial periods (Fig. 7; Alloway et al., 2007). Additionally, the greater sediment flux to the ocean during glacials, driven by lower sea levels (Lambeck et al., 2014; Dutton et al., 2015; Spratt and Lisiecki, 2016) and increased hinterland erosion (McGlone, 2001; Upton et al., 2013; Woodhouse et al., 2024), would have led to greater pollen dilution compared to interglacial periods (Figs. 6 and 7). Therefore these two factors would be interplaying to increase pollen concentration in interglacial periods and decrease pollen concentration in glacial periods. The relationship between pollen concentration and SAR cannot be examined over the glacial–interglacials in ODP-1123B because the pollen was too sparse to calculate concentration (see Section 2). However this point alone tells us that the pollen concentration is extremely low and alongside the low SAR, indicates that very little terrestrial material is reaching this distal site (Figs. 1 and 6).

4.3. Comparisons to other terrestrial and marine records

In Aotearoa-New Zealand, most continuous terrestrial pollen records do not extend to the LGM, and although they do not extend as far back as deep-marine records, they still allow for a broad comparison of warmer interglacial and cooler glacial intervals between terrestrial and deep-marine records. Wilmshurst et al. (1999) shows detailed comparisons between terrestrial (Repongaere Swamp) and shallow marine (W369) records in Poverty Bay, Aotearoa-New Zealand, with records extending back to the late Holocene (Fig. 1). In the terrestrial record podocarps and hardwoods were ~80% which is comparable to the average percentages in the deep-marine cores P69/MD97-2121 (83%), IODP-U1520D (82%) and ODP-1123B (81%; Table 2; Wilmshurst et al., 1999). The marine core W396 had lower podocarp-hardwood pollen (mean=64%), as well as lower small tree, shrub, herb and grass pollen (i.e. mean *Coprosma*= 9.4% terrestrial, 0.3% marine), which they attributed to these taxa being locally abundant around the terrestrial site (Wilmshurst et al., 1999). Overall, the deep-marine records pollen assemblages more closely follow the assemblages in the terrestrial Repongaere Swamp core during interglacials than the shallow-marine W396 core, which could be due to the shallow-marine environment being a higher energy environment, causing pollen to winnow out (Table 2; Wilmshurst et al., 1999). Newnham and Lowe, 2000 found similar percentages of podocarp taxa in the Kaipo Bog sediment core

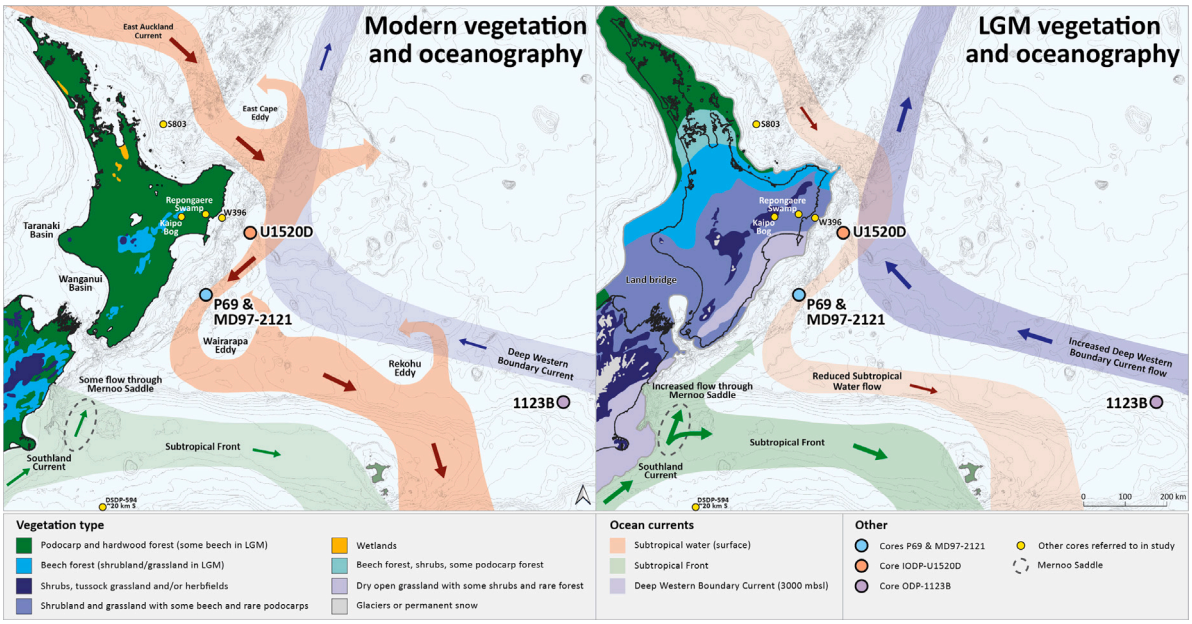

Fig. 7. Modern and LGM vegetation cover and ocean currents inferred for northeastern Aotearoa-New Zealand. Vegetation and LGM ocean currents are adapted from Alloway et al. (2007), with additional ocean current information from Nelson et al. (2000), Bostock et al. (2015), and Chiswell et al. (2015).

(Fig. 1) in the Holocene Optimum (~11.14 ka) with taxa such as *D. cupressinum* and *P. taxifolia* reaching as high as 35% and 45% respectively, again showing the similarities between interglacial terrestrial records from the eastern North Island and the deep-marine cores (Alloway et al., 2007). Mildenhall and Orpin (2010) analysed multiple pollen records from the Waipaoa Sedimentary System and found that in the LGM podocarps-hardwoods-beech combined averaged 35%, and small trees and shrubs and herbs and grasses averaged 15% and 40%, respectively. During glacials the percentage of small trees and shrubs in P69/MD97-2121, IODP-U1520D, and ODP-1123B was similar to Mildenhall and Orpin (2010), but the combined podocarps-hardwoods-beech was much higher (>66% in the deep-marine records), while herbs and grasses were approximately four times lower (Table 2). Overall, these comparisons between the deep-marine cores and to other terrestrial and marine records from northern Aotearoa-New Zealand show that pollen assemblages are generally similar during interglacial periods but diverge during glacial periods.

4.4. Drivers of glacial and interglacial pollen assemblage variations in the deep-marine records

In interglacial periods, much of the northern South Island and North Island of Aotearoa-New Zealand was covered in podocarp-hardwood forests, with beech forests and shrub/grasslands at higher elevations (i.e. Taupō Volcanic Zone; Fig. 7; Alloway et al., 2007). This uniformity of the vegetation of the northern South Island and the North Island could explain why the pollen assemblages in the deep-marine cores in interglacial periods are similar within and between cores (Wilmshurst et al., 1999; Newnham and Lowe, 2000; McGlone, 2001; Mildenhall et al., 2004; Mildenhall and Orpin, 2010).

During the LGM, lower sea levels (~134 m lower; Lambeck et al., 2014; Dutton et al., 2015; Spratt and Lisiecki, 2016) created a land bridge which connected the North and South Islands (Trewick and Bland, 2012; Bland et al., 2024), resulting in a greater subaerial landmass in Aotearoa-New Zealand at lower altitudes, particularly around the low-lying Wanganui and Taranaki basins (Fig. 7). In contrast to the relatively homogeneous interglacial vegetation in Aotearoa-New Zealand, the vegetation in the connected South–North Island was much more heterogeneous in the LGM (Fig. 7; Alloway et al., 2007; Trewick and Bland, 2012; Newnham et al., 2013). As the climate cooled during the last glacial period, podocarp-hardwood and beech forests remained continuous in the northern North Island and contracted into smaller communities in the south where shrub, herb, and grasslands expanded and became dominant (Fig. 7; McGlone, 1985; Alloway et al., 2007; McGlone et al., 2010; Newnham et al., 2013; Wood et al., 2017). Around the land bridge and the northern South Island, the vegetation was similar to the central North Island, with shrublands, grasslands, and some beech forest at lower elevations, and herbfields and tussocks at higher elevations (Fig. 7; Alloway et al., 2007; Trewick and Bland, 2012; Newnham et al., 2013). The consequent glacial vegetation in these regions of Aotearoa-New Zealand was a mosaic of different vegetation types, meaning that if each deep-marine core has a slightly different source area, the pollen assemblages could vary significantly between records (Fig. 7).

In addition to the vegetation in Aotearoa-New Zealand changing during glacial periods, the position of water masses and ocean currents also varied (Fig. 7; Nelson et al., 2000; Hall et al., 2001, 2002; Alloway et al., 2007; Crundwell et al., 2008; Bostock et al., 2015; Lorrey and Bostock, 2017). During the LGM, the Subtropical Front is believed to have remained in a similar position to today, due to the bathymetric constraint of the Chatham Rise (Fig. 7; Weaver et al., 1998; Nelson et al., 2000; Schaefer et al., 2005; Bostock et al., 2015; Chiswell et al., 2015). The southward flow of STW through currents like the ECC is known to have been weaker and it has been proposed that during the LGM there was a jet of Subantarctic Water that travelled north through the Mernoo Saddle (present day=55 km wide, 550 m deep), at the western edge of the Chatham Rise (Fig. 7; Weaver et al., 1998; Nelson et al., 2000; Bostock et al., 2015; Lorrey and Bostock, 2017). At intermediate depths, the southward flowing AAIW is thought to have remained relatively stable, while in the deep ocean, the northward-flowing DWBC is thought to have been stronger during the LGM (Fig. 7; Hall et al., 2001, 2002). The combination of changes in the distribution of vegetation in Aotearoa-New Zealand and the changes in the ocean currents could explain the different glacial pollen assemblages in the three cores (Fig. 7; Table 2). For example, the lower podocarp and hardwood pollen in P69/MD97-2121 during glacials could be a result of the reduced flow

of STW, bringing less podocarp pollen from the north (Fig. 7), and an increased flow of Subantarctic Water through the Mernoo Saddle, causing P69/MD97-2121 to exhibit a more southern pollen signal than the other two cores.

Regardless of the underlying cause of the differences in glacial pollen assemblages, an important question is how much these variations in deep-marine cores could influence the final interpretation of past vegetation. The interglacial vegetation signal across the deep-marine cores would show the same vegetation signal of a warmer climate, with dominant podocarp and hardwood forests and lesser beech, small trees and shrubs, and herbs and grasses (Fig. 7; McGlone, 2001; Mildenhall, 2003; Mildenhall et al., 2004; Alloway et al., 2007). In glacial periods the overall interpretation of past climate in the three cores would be the same: cooler with reduced podocarp-hardwood forests, and increased beech forest, shrublands, and grasslands (Figs. 4 and 7; Table 2; McGlone, 2001; Mildenhall, 2003; Mildenhall et al., 2004; Alloway et al., 2007; Newnham et al., 2013). However, due to the differences in the glacial pollen assemblages, one could interpret P69/MD97-2121 as indicative of a cooler climate than IODP-U1520D and ODP-1123B, given the lower percentage of podocarps and hardwoods and the increased proportions of other taxa like beech, small trees and shrubs, and herbs and grasses (Table 2). For accurate vegetation reconstructions from deep-marine pollen records, it is crucial to understand and account for transport mechanisms to different sites and how these processes may vary and bias the pollen records over glacial–interglacial cycles.

4.5. Benefits and considerations for using deep-marine pollen records

As shown in this study, deep-marine pollen records can be used to create high-quality records of past vegetation and can extend further back than most terrestrial records (Dupont, 1999; Sánchez-Goñi et al., 2018). Instead of capturing a local vegetation signal, as lake and swamp records do, marine pollen records capture a regional vegetation signal which may also be more representative of a regional palaeoclimate signal. The three cores P69/MD97-2121, IODP-U1520D, and ODP-1123B show that although the transport pathways of pollen to reach the deep ocean can be long and complex, the pollen records from these sedimentary records are surprisingly consistent. Furthermore, the IODP-U1520D record shows that sampling sedimentary records that are dominated by turbidites can still give us a reliable picture of past vegetation. This has similarly been found in studies of the UK North Sea fans (Vieira and Jolley, 2020; Jolley et al., 2022) where sampling of deep-marine turbidites allowed them to reconstruct vegetation changes across the Palaeocene-Eocene Thermal Maximum. Similarly, Beaudouin et al. (2004) reconstructed palaeovegetation since MIS3 by sampling turbidites from a deep-marine core from the Gulf of Lions, and found that pollen was abundant in turbidite facies and almost absent from hemipelagic facies in the core. In contrast, McGann (2018) found that the pollen assemblages in turbidites were biased with higher percentages of hydrologically efficient grains compared to the background sediments in their core from the Ascension-Monterey Canyon system. Although our study shows that deep-marine turbidite records can create accurate records of past vegetation like Beaudouin et al. (2004), Vieira and Jolley (2020) and Jolley et al. (2022), the repeating pollen sequence in IODP-U1520D shows that when we are using records from active margins, we need to interpret the past vegetation with caution and utilise other proxies (i.e. $\delta^{18}O$, grain-size analysis) to disentangle signals of vegetation change from other processes including Mass Transport Deposits (Fig. B.8). Despite this, the similarity of the turbidite-dominated IODP-U1520D record to P69/MD97-2121 is surprising. The short turbidite recurrence interval (one bed every ~33-237 years in Shorrock et al. 2025) in IODP-U1520D shows that turbidity currents were frequent enough and that sediment and pollen were being transported to the deep ocean regularly. Understanding the bed recurrence interval is important as it provides a rough estimate of how quickly sediment and pollen are transported to the deep ocean (see Beaudouin et al., 2004). In IODP-U1520D, the short turbidite recurrence interval provides a high resolution and near continuous palaeovegetation record, which can be extended further back in time to answer questions about key climate intervals like the Mid-Pleistocene Transition (Herbert, 2023; Crundwell and Woodhouse, 2024a), for which very few vegetation records exist in Aotearoa-New Zealand. We suggest that similar palaeovegetation records could be obtained from sediment cores with frequent turbidites from active margins around the globe, including the Nankai Trench (Underwood and Pickering, 2018), Chile Trench (Blumberg et al., 2008), Makran Trench (Bourget et al., 2010), Cascadia Basin Underwood et al. (2005), and Sunda Trench (Pickering et al., 2020), to name a select few.

To reconstruct past vegetation by using pollen in sediment cores, maximising pollen recovery is essential, making it important to consider sediment accumulation rates and potential dilution of pollen by sediment. If we consider ODP-1123B and IODP-U1520D as end members on a sedimentation rate scale, P69/MD97-2121 is in the "goldilocks zone" (Fig. 6). The sedimentation is just high enough that considerable amounts of terrestrial sediment and pollen are deposited at this deep-marine site (where not enough terrestrial material is reaching ODP-1123B), but not diluting the pollen concentrations too much, as we see in IODP-U1520D (Fig. 6). Therefore, when choosing a deep-marine record for vegetation reconstructions, a SAR of 0.05–0.2 m/ka of fine (clay-silt) terrigenous sediment would likely provide good pollen recovery. Additionally, selecting a proximal deep-marine core site from the slope or adjacent abyssal plain that receives sufficient terrigenous material, whether from a river (or canyon systems linked to rivers), increases the likelihood of recovering high concentrations of pollen. Cores distal to land, like ODP-1123B, can yield pollen records, but low pollen recovery (Mildenhall, 2003) due to limited terrestrial input makes them more challenging to analyse than land-proximal cores (i.e. <100 km; Fig. 6).

5. Conclusion

This study demonstrates that deep-marine pollen records from varying depths, distances from land, sedimentary settings, and inferred pollen transport processes all show consistent patterns of regional vegetation change. We find that the deep-marine records from the east coast of Aotearoa-New Zealand show close similarities in interglacial periods and diverge in glacial periods, which we attribute to the less homogeneous vegetation in the North Island and changing ocean current regimes in glacial periods (Fig. 7; Table 2). Deep-marine pollen records are a powerful tool for understanding long-term vegetation change (Dupont, 1999; Sánchez-Goñi et al., 2018), offering a regional perspective on past ecosystems in deeper time periods. However, these records must be interpreted with caution, as understanding the sedimentary processes and transport mechanisms is essential for developing robust reconstructions of past vegetation and climate. We find that sedimentary sequences with sediment accumulation rates between 0.05–0.2 m/ka of fine (clay-silt) sediment, in land-proximal (<100 km) sites yield the best pollen recovery, which can be applied when selecting new core sites or using legacy cores for palaeovegetation reconstructions. We also suggest that sampling pollen from turbidites in deep-marine records can yield reliable palaeovegetation records, giving us the ability to create long palaeoclimate records from active margins, where in the past, palynological studies for palaeoclimate reconstruction would not have been attempted. We suggest that this methodology can be applied to turbidite-dominated records from active margins globally (Underwood et al., 2005; Blumberg et al., 2008; Bourget et al., 2010; Underwood and Pickering, 2018; Pickering et al., 2020).

CRediT authorship contribution statement

Laura S. McDonald: Writing – review & editing, Writing – original draft, Visualization, Project administration, Methodology, Investigation, Formal analysis, Data curation, Conceptualization. **Lorna J. Strachan:** Writing – review & editing, Supervision, Funding acquisition, Conceptualization. **Katherine Holt:** Writing – review & editing, Supervision, Resources, Methodology, Conceptualization. **Adam D. McArthur:** Writing – review & editing, Supervision, Conceptualization. **Anthony E. Shorrock:** Writing – review & editing, Investigation, Formal analysis. **Martin P. Crundwell:** Resources, Investigation. **Katharina Pank:** Writing – review & editing, Resources, Investigation. **Madison Clarke:** Writing – review & editing, Investigation. **Adam Woodhouse:** Investigation. **Davide Gamboa:** Writing – review & editing, Investigation. **Jenni L. Hopkins:** Writing – review & editing, Resources. **Matt S. McGlone:** Writing – review & editing. **Helen C. Bostock:** Writing – review & editing, Supervision, Conceptualization.

Acknowledgements and funding

We acknowledge and thank Dallas Mildenhall for the pollen data from MD97-2121 and for his encouragement on this manuscript. We appreciate the useful discussions from the Hikurangi Marsden Group, particularly Phil Barnes, Steffen Kutterolf, and Kathie Marsaglia. We also thank Paul Augustinus, David Wackrow, Natalia Abrego, and Hoa Nguyen for sediment and pollen processing help and advice. We also thank Massey University, Palmerston North, for the use of the palynology laboratory. Funding for this project is from the Marsden Fund of the Royal Society Te Apārangi (PI Lorna Strachan, 20-UOA-099). Davide Gamboa thanks funding by national funds through FCT – Fundação para a Ciência e a Tecnologia I.P., under the project/grant UID/50006 + LA/P/0094/2020 (doi.org/10.54499/LA/P/0094/2020). Open-access publishing is facilitated by The University of Auckland, as a part of the Elsevier and University of Auckland agreement.

Declaration of competing interest

The authors declare that they have no known competing financial interests or personal relationships that could have appeared to influence the work reported in this paper.

Appendix A. Supplementary tables

See Table A.3.

Appendix B. Supplementary figures

See Fig. B.8.

Data availability

The data that support the findings of this study are openly available on Zenodo at https://doi.org/10.5281/zenodo.16623457.

Table A.3
Summary of age inputs into the updated IODP-U1520D age model.

Age type	Number of dates/tie points	Depth range (mbsf)	Authors
Radiocarbon	8	5–106	Woodhouse et al. (2024)
Foraminifera biostratigraphy	9	6.2–186.2	Crundwell and Woodhouse (2024a,b)
Tephrochronology	10	1.2–187.5	Pank et al. (2025), Clarke (2023)
δ^{18}O *Uvigerina peregrina*	87	5.9–189.3	Noda et al. (2024), Woodhouse et al. (2024), this paper

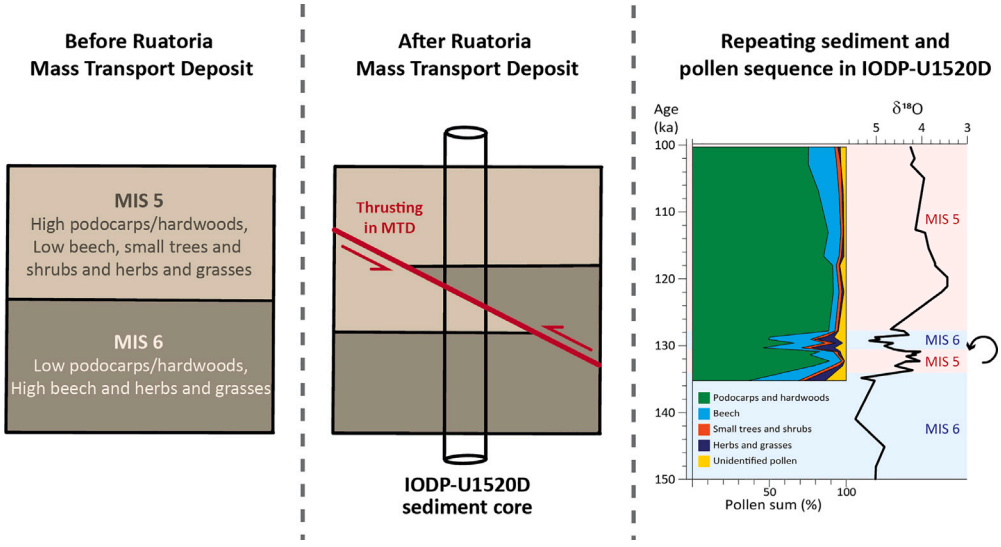

Fig. B.8. Thrust faulting from the Ruatōria Mass Transport Deposit as a potential explanation for the repeating pollen and δ^{18}O sequence in IODP-U1520D during the MIS6-5 transition.

References

Abell, J.M., Pingram, M.A., Özkundakci, D., David, B.O., Scarsbrook, M., Wilding, T., Williams, A., Noble, M., Brasington, J., Perrie, A., 2023. Large floodplain river restoration in New Zealand: synthesis and critical evaluation to inform restoration planning and research. Reg. Environ. Chang. 23 (18).

Alloway, B.V., Lowe, D.J., Barrell, D.J., Newnham, R.M., Almond, P.C., Augustinus, P.C., Bertler, N.A., Carter, L., Litchfield, N.J., McGlone, M.S., et al., 2007. Towards a climate event stratigraphy for New Zealand over the past 30 000 years (NZ-INTIMATE project). J. Quat. Sci. 22, 9–35.

Alsop, G., Marco, S., Weinberger, R., Levi, T., 2024. A new mechanism to repeat stratigraphic sequences during gravity-driven extension. J. Struct. Geol. 105184.

Anderson, H.J., Pedro, J.B., Bostock, H.C., Chase, Z., Noble, T.L., 2020. Recalibrated age model and sea surface temperatures of sediment core MD97-2121. In: Anderson, HJ, Others (2020): 14 Southern Ocean Sea Surface Temperature Records Recalibrated To MARINE20 and Tied To the AICC2012 Timescale, Southern Ocean Sea Surface Temperature Anomaly Stacks [Dataset Bundled Publication. PANGAEA, http://dx.doi.org/10.1594/PANGAEA.912146.

Augustinus, P., D'costa, D., Deng, Y., Hagg, J., Shane, P., 2011. A multi-proxy record of changing environments from ca. 30 000 to 9000 cal. a BP: Onepoto maar palaeolake, Auckland, New Zealand. J. Quat. Sci. 26, 389–401.

Bailey, W.S., McArthur, A.D., McCaffrey, W.D., 2021. Distribution of contourite drifts on convergent margins: Examples from the Hikurangi subduction margin of New Zealand. Sedimentology 68, 294–323.

Barnes, P., Wallace, L., Saffer, D., Pecher, I., Petronotis, K., LeVay, L., Bell, R., Crundwell, M., Engelmann de Oliveira, C., Fagereng, A., et al., 2019. Proceedings of the International Ocean Discovery Program Volume 372B/375: Site U1520. In: Proceedings of the International Ocean Discovery Program. IODP, pp. 1–76.

Barrell, D.J., Almond, P.C., Vandergoes, M.J., Lowe, D.J., Newnham, R.M., INTIMATE members, 2013. A composite pollen-based stratotype for inter-regional evaluation of climatic events in New Zealand over the past 30 000 years (NZ-INTIMATE project). Quat. Sci. Rev. 74, 4–20.

Beaudouin, C., Dennielou, B., Melki, T., Guichard, F., Kallel, N., Berné, S., Huchon, A., 2004. The Late-Quaternary climatic signal recorded in a deep-sea turbiditic levee (Rhône Neofan, Gulf of Lions, NW Mediterranean): palynological constraints. Sediment. Geol. 172, 85–97.

Beaufort, L., Chen, M.T., Chivas, A., Manighetti, B., 1997. IPHIS-IMAGES ill/MD 106 campaign from 05-23-97 to 06-28-97. In: Publications of the French Institute for Polar Research and Technology. Reports from campaigns to the sea.

Bland, K.J., Strogen, D.P., Arnot, M.J., Viskovic, G.P.D., Sahoo, T.R., Seebeck, H., Kellett, R., Bull, S., Thrasher, G.P., Kroeger, K.F., Lawrence, M.J.F., Griffin, A.G., 2024. New Zealand's offshore sedimentary basins. N. Z. J. Geol. Geophys. 1–34.

Blumberg, S., Lamy, F., Arz, H.W., Echtler, H., Wiedicke, M., Haug, G.H., Oncken, O., 2008. Turbiditic trench deposits at the South-Chilean active margin: a Pleistocene–Holocene record of climate and tectonics. Earth Planet. Sci. Lett. 268, 526–539.

Bostock, H.C., Hayward, B.W., Neil, H.L., Sabaa, A.T., Scott, G.H., 2015. Changes in the position of the Subtropical Front south of New Zealand since the last glacial period. Paleoceanography 30, 824–844.

Bostock, H., Jenkins, C., Mackay, K., Carter, L., Nodder, S., Orpin, A., Pallentin, A., Wysoczanski, R., 2019. Distribution of surficial sediments in the ocean around New Zealand/Aotearoa. Part B: continental shelf. N. Z. J. Geol. Geophys. 62, 24–45.

Bostock, H.C., Sutton, P.J., Williams, M.J., Opdyke, B.N., 2013. Reviewing the circulation and mixing of Antarctic Intermediate Water in the South Pacific using evidence from geochemical tracers and Argo float trajectories. Deep. Sea Res. Part I: Ocean. Res. Pap. 73, 84–98.

Bourget, J., Zaragosi, S., Ellouz-Zimmermann, S., Ducassou, E., Prins, M., Garlan, T., Lanfumey, V., Schneider, J.L., Rouillard, P., Giraudeau, J., 2010. Highstand vs. lowstand turbidite system growth in the Makran active margin: Imprints of high-frequency external controls on sediment delivery mechanisms to deep water systems. Mar. Geol. 274, 187–208.

Bull, S., Arnot, M., Browne, G., Crundwell, M., Nicol, A., Strachan, L., 2019. Neogene and Quaternary Mass-Transport Deposits From the Northern Taranaki Basin (North Island, New Zealand) Morphologies, Transportation Processes, and Depositional Controls. In: Submarine Landslides: Subaqueous Mass Transport Deposits from Outcrops To Seismic Profiles. pp. 171–180.

Camp, S.L., 2020. Going With The Flow: Understanding Sedimentary Processes on the Hawke Bay Continental Slope. Master's thesis. The University of Auckland.

Campbell, J., Fletcher, W., Hughes, P., Shuttleworth, E., 2016. A comparison of pollen extraction methods confirms dense-media separation as a reliable method of pollen preparation. J. Quat. Sci. 31, 631–640.

Cardona, S., Wood, L.J., Dugan, B., Jobe, Z., Strachan, L.J., 2020. Characterization of the Rapanui mass-transport deposit and the basal shear zone: Mount Messenger Formation, Taranaki Basin, New Zealand. Sedimentology 67, 2111–2148.

Carter, L., Manighetti, B., 2006. Glacial/interglacial control of terrigenous and biogenic fluxes in the deep ocean off a high input, collisional margin: A 139 kyr-record from New Zealand. Mar. Geol. 226, 307–322.

Carter, L., Manighetti, B., Elliot, M., Trustrum, N., Gomez, B., 2002. Source, sea level and circulation effects on the sediment flux to the deep ocean over the past 15 ka off eastern New Zealand. Glob. Planet. Change 33, 339–355.

Carter, L., McCave, I., 1997. The sedimentary regime beneath the deep western boundary current inflow to the southwest Pacific Ocean. J. Sediment. Res. 67, 1005–1017.

Carter, R.M., Richter, C., Riegel, R.N., 1999. Proceedings of the Ocean Drilling Program: covering Leg 181 of the cruises of the Drilling Vessel JOIDES Resolution, Sydney, Australia to Wellington, New Zealand, Sites 1119-1125, 11 August-8 1998. Initial reports, Southwest Pacific Gateways. In: Proceedings of the Ocean Drilling Program. Texas A & M University, pp. 1–80.

Chiswell, S.M., 2005. Mean and variability in the Wairarapa and Hikurangi eddies, New Zealand. N. Z. J. Mar. Freshw. Res. 39, 121–134.

Chiswell, S.M., Bostock, H.C., Sutton, P.J., Williams, M.J., 2015. Physical oceanography of the deep seas around New Zealand: a review. N. Z. J. Mar. Freshw. Res. 49, 286–317.

Clare, M.A., Clarke, J.H., Talling, P.J., Cartigny, M.J., Pratomo, D., 2016. Preconditioning and triggering of offshore slope failures and turbidity currents revealed by most detailed monitoring yet at a fjord-head delta. Earth Planet. Sci. Lett. 450, 208–220.

Clark, K., Nissen, E., Howarth, J., Hamling, I., Mountjoy, J., Ries, W., Jones, K., Goldstien, S., Cochran, U., Villamor, P., et al., 2017. Highly variable coastal deformation in the 2016 Mw7.8 Kaikōura, New Zealand, Earthquake reflects rupture complexity along a transpressional plate boundary. Earth Planet. Sci. Lett. 474, 334–344.

Clarke, M., 2023. Cryptotephra studies applied to a deep marine sedimentary record in the northern Hikurangi Trough, Aotearoa New Zealand. Master's thesis. Te Herenga Waka-Victoria University of Wellington.

Collot, J.Y., Lewis, K., Lamarche, G., Lallemand, S., 2001. The giant Ruatoria debris avalanche on the northern Hikurangi margin, New Zealand: Result of oblique seamount subduction. J. Geophys. Res.: Solid Earth 106, 19271–19297.

Crouch, E., Mildenhall, D., Neil, H., 2010. Distribution of organic-walled marine and terrestrial palynomorphs in surface sediments, offshore eastern New Zealand. Mar. Geol. 270, 235–256.

Crundwell, M.P., Scott, G., Naish, T., Carter, L., 2008. Glacial–interglacial ocean climate variability from planktonic foraminifera during the Mid-Pleistocene transition in the temperate Southwest Pacific, ODP Site 1123. Palaeogeogr. Palaeoclimatol. Palaeoecol. 260, 202–229.

Crundwell, M.P., Woodhouse, A., 2024a. Biostratigraphically constrained chronologies for Quaternary sequences from the Hikurangi margin of north-eastern Zealandia. N. Z. J. Geol. Geophys. 67, 364–384.

Crundwell, M.P., Woodhouse, A., 2024b. A detailed biostratigraphic framework for 0–1.2 Ma Quaternary sediments of north-eastern Zealandia. N. Z. J. Geol. Geophys. 67, 350–363.

Dodson, J., 1976. Modern pollen spectra from Chatham Island, New Zealand. N. Z. J. Bot. 14, 341–347.

Dupont, L., 1999. Pollen and spores in marine sediments from the east Atlantic-A view from the ocean into the African Continent. In: Use of Proxies in Paleoceanography: Examples from the South Atlantic. Springer, pp. 523–546.

Dupont, L., 2011. Orbital scale vegetation change in Africa. Quat. Sci. Rev. 30, 3589–3602.

Dutton, A., Carlson, A.E., Long, A.J., Milne, G.A., Clark, P.U., DeConto, R., Horton, B.P., Rahmstorf, S., Raymo, M.E., 2015. Sea-level rise due to polar ice-sheet mass loss during past warm periods. Science 349, aaa4019.

Elliot, M., Manighetti, B., Carter, L., 2003. In the beginning—high resolution evidence from a deep ocean core for the early settlement of New Zealand. In: Gao, J., Le Heron, R., Logie, J. (Eds.), Windows on a Changing World. Proceedings of the 22nd New Zealand Geographical Society Conference. In: New Zealand Geographical Society Conference Series, pp. 92–96.

Faegri, K., Kaland, P.E., Krzywinski, K., et al., 1989. Textbook of pollen analysis, fourth ed. John Wiley & Sons Ltd.

Gamboa, D., Barnes, P., Bell, R., Moore, G., Mountjoy, J., Paganoni, M., Clennel, M., Cook, A., McNamara, D., Underwood, M., et al., 2019. Revisiting the giant Ruatoria Debris Flow on the Hikurangi Margin, New Zealand: results from IODP Expeditions 372 and 375, Site U1520. Geophys. Res. Abstr. 1–1.

GNS Science, 2024. New Zealand fossil record file. Datasets: SE40177/f0001, SW41171/f0002. http://dx.doi.org/10.21420/JQQB-NK89.

González, C., Dupont, L.M., Behling, H., Wefer, G., 2008. Neotropical vegetation response to rapid climate changes during the last glacial period: Palynological evidence from the Cariaco Basin. Quat. Res. 69, 217–230.

Grimm, E.C ., 2020. Tilia. Version 3.0.1.

Guilderson, T.P., Reimer, P.J., Brown, T.A., 2005. The boon and bane of radiocarbon dating. Science 307, 362–364.

Hall, I.R., Carter, L., Harris, S.E., 2002. Major depositional events under the deep Pacific inflow. Geology 30, 487–490.

Hall, I.R., McCave, I.N., Shackleton, N.J., Weedon, G.P., Harris, S.E., 2001. Intensified deep Pacific inflow and ventilation in Pleistocene glacial times. Nature 412, 809–812.

Hamling, I.J., Hreinsdóttir, S., Clark, K., Elliott, J., Liang, C., Fielding, E., Litchfield, N., Villamor, P., Wallace, L., Wright, T.J., et al., 2017. Complex Multifault Rupture During the 2016 Mw 7.8 Kaikōura, New Zealand, Earthquake. Science 356, Eaam7194.

Hammer, Ø., Harper, D.A., 2001. PAST: Paleontological Statistics Software Package for Education and Data Analysis. Palaeontol. Electron. 4, 1.
Hayward, B.W., Sabaa, A.T., Howarth, J.D., Orpin, A.R., Strachan, L.J., 2022. Foraminiferal evidence for the provenance and flow history of turbidity currents triggered by the 2016 Kaikōura Earthquake. N. Z. J. Geol. Geophys. 1–14.
Heaton, T.J., KÖhler, P., Butzin, M., Bard, E., Reimer, R.W., Austin, W.E., Ramsey, C.B., Grootes, P.M., Hughen, K.a., Kromer, B., Others, 2020. Marine20—the marine radiocarbon age calibration curve (0–55, 000 cal bp). Radiocarbon 62, 779–820.
Herbert, T.D., 2023. the Mid-Pleistocene Climate Transition. Annu. Rev. Earth Planet. Sci. 51, 389–418.
Heusser, L.E., Balsam, W.L., 1977. Pollen distribution in the northeast Pacific Ocean. Quat. Res. 7, 45–62.
Heusser, L.E., Van de Geer, G., 1994. Direct Correlation of Terrestrial and Marine Paleoclimatic Records from Four Glacial-Interglacial Cycles—DSDP Site 594 Southwest Pacific. Quat. Sci. Rev. 13, 273–282.
Heusser, L.E., Heusser, C., Pisias, N., 2006. Vegetation and Climate Dynamics of Southern Chile During the Past 50 000 years: Results of ODP Site 1233 Pollen Analysis. Quat. Sci. Rev. 25, 474–485.
Hicks, D.M., Shankar, U., McKerchar, a.I., Basher, L., Lynn, I., Page, M., Jessen, M., 2011. Suspended Sediment Yields from New Zealand Rivers. J. Hydrol. (New Zealand) 50, 81–142.
Holmes, P.L., 1990. Differential transport of spores and pollen: A laboratory study. Rev. Palaeobot. Palynol. 64, 289–296.
Holt, K.A., Wallace, R.C., Neall, V.E., Kohn, B.P., Lowe, D.J., 2010. Quaternary tephra marker beds and their potential for palaeoenvironmental reconstruction on Chatham Island, east of New Zealand, southwest Pacific Ocean. J. Quat. Sci. 25, 1169–1178.
Hooghiemstra, H., 2023. Making a long continental pollen record, a fabulous and bizarre enterprise: a 50-year retrospective. Palynology 47, 2191257.
Hooghiemstra, H., Stalling, H., Agwu, C.O., Dupont, L.M., 1992. Vegetational and climatic changes at the northern fringe of the Sahara 250,000–5000 years BP: evidence from 4 marine pollen records located between Portugal and the Canary Islands. Review Palaeobot. Palynol. 74, 1–53. http://dx.doi.org/10.1016/0034-6667(92)90012-4.
Howarth, J.D., Orpin, A.R., Kaneko, Y., Strachan, L.J., Nodder, S.D., Mountjoy, J.J., Barnes, P.M., Bostock, H.C., Holden, C., Jones, K., et al., 2021. Calibrating the marine turbidite palaeoseismometer using the 2016 Kaikōura earthquake. Nat. Geosci. 14, 161–167.
Hume, T.M., Herdendorf, C.E., 1988. A geomorphic classification of estuaries and its application to coastal resource management—a New Zealand example. Ocean. Shorel. Manag. 11, 249–274.
Hume, T.M., Snelder, T., Weatherhead, M., Liefting, R., 2007. A controlling factor approach to estuary classification. Ocean & Coastal Management 50, 905–929.
Igarashi, Y., Oba, T., 2006. Fluctuations in the East Asian monsoon over the last 144 ka in the northwest Pacific based on a high-resolution pollen analysis of IMAGES core MD01-2421. Quat. Sci. Rev. 25, 1447–1459.
Jolley, D., Vieira, M., Jin, S., Kemp, D.B., 2022. Palynofloras, palaeoenvironmental change and the inception of the Paleocene Eocene Thermal Maximum; the record of the Forties Fan, Sele Formation, North Sea Basin. J. Geol. Soc. 180, jgs2021–131.
Kershaw, P., Kaars, S.Van.Der., 2006. Pollen records, late Pleistocene: Australia and New Zealand. In: Encyclopedia of Quaternary Science. Elsevier-WB Saunders, pp. 2613–2623.
Kershaw, A.P., Kaars, S.van.der., Moss, P.T., 2003. Late Quaternary Milankovitch-scale climatic change and variability and its impact on monsoonal Australasia. Mar. Geol. 201, 81–95.
Lambeck, K., Rouby, H., Purcell, A., Sun, Y., Sambridge, M., 2014. Sea level and global ice volumes from the Last Glacial Maximum to the Holocene. Proc. Natl. Acad. Sci. 111, 15296–15303.
Large, M.F., Braggins, J.E., 1991. Spore atlas of New Zealand ferns & fern allies. Sir Pub.
Lee, T., Rand, D., Lisiecki, L.E., Gebbie, G., Lawrence, C., 2023. Bayesian age models and stacks: combining age inferences from radiocarbon and benthic δ18O stratigraphic alignment. Clim. the Past 19, 1993–2012.
Lewis, K., 1994. The 1500-km-long Hikurangi Channel: trench-axis channel that escapes its trench, crosses a plateau, and feeds a fan drift. Geo-Marine Lett. 14, 19–28.
Lewis, K.B., Barnes, P.M., 1999. The 1500-km-long Hikurangi Channel: trench-axis channel that escapes its trench, crosses a plateau, and feeds a fan drift. Mar. Geol. 162, 39–69.
Lewis, K.B., Collot, J.Y., Lallem, S.E., 1998. The dammed Hikurangi Trough: a channel-fed trench blocked by subducting seamounts and their wake avalanches (New Zealand–France GeodyNZ Project). Basin Res. 10, 441–468.
Lewis, K.B., Pantin, H.M., 2002. Channel-axis, overbank and drift sediment waves in the southern Hikurangi Trough, New Zealand. Mar. Geol. 192, 123–151.
Lewis, K., Pettinga, J., 1993. The emerging, imbricate frontal wedge of the Hikurangi Margin. Sediment. Basins the World 2, 225–250.
Li, W., Li, X., Mei, X., Zhang, F., Xu, J., Liu, C., Wei, C., Liu, Q., 2021. A review of current and emerging approaches for Quaternary marine sediment dating. Sci. Total Environ. 780, 146522.
Lisiecki, L.E., Raymo, M.E., 2005. A Pliocene-Pleistocene stack of 57 globally distributed benthic δ18O records. Paleoceanography 20.
Litchfield, N.J., Villamor, P., Dissen, R.J.V., Nicol, A., Barnes, P.M., A. Barrell, D.J., Pettinga, J.R., Langridge, R.M., Little, T.A., Mountjoy, J.J., et al., 2018. Surface rupture of multiple crustal faults in the 2016 Mw 7.8 Kaikōura, New Zealand, Earthquake. In: Bulletin of the Seismological Society of America. vol. 108, pp. 1496–1520.
Lorrey, A., Bostock, H., 2017. The climate of New Zealand through the Quaternary. Landsc. Quat. Environ. Chang. N. Z. 6, 7–139.
Lunenburg, R., 2017. Characterisation of sediment gravity flow processes in the Tuaheni Canyon, Poverty Bay, New Zealand. Master's thesis. The University of Auckland.
Lyle, M., Heusser, L., Herbert, T., Mix, A., Barron, J., 2001. Interglacial theme and variations: 500 ky of orbital forcing and associated responses from the terrestrial and marine biosphere, US Pacific Northwest. Geology 29 (12), 1115–1118.
Maier, K.L., Strachan, L.J., Tickle, S., Orpin, A.R., Nodder, S.D., Howarth, J., 2024. Testing turbidite conceptual models with the Kaikōura Earthquake co-seismic event bed, Aotearoa New Zealand. J. Sediment. Res. 94 (3), 325–333.
McArthur, A.D., Crisóstomo-Figueroa, A., Wunderlich, A., Karvelas, A., McCaffrey, W.D., 2022. Sedimentation on structurally complex slopes: Neogene to recent deep-water sedimentation patterns across the central Hikurangi subduction margin, New Zealand. Basin Res. 34, 1807–1837.
McArthur, A., Gamberi, F., Kneller, B., Wakefield, M., Souza, P., Kuchle, J., 2017. Palynofacies classification of submarine fan depositional environments: Outcrop examples from the Marnoso-Arenacea Formation, Italy. Mar. Pet. Geol. 88, 181–199.
McCave, I., Carter, L., 1997. Recent sedimentation beneath the deep Western Boundary Current off northern New Zealand. Deep. Sea Res. Part I: Ocean. Res. Pap. 44, 1203–1237.
McDonald, L.S., Strachan, L.J., Holt, K., McArthur, A.D., Barnes, P.M., Maier, K.L., Orpin, A.R., Horrocks, M., Ganguly, A., Hopkins, J.L., Bostock, H.C., 2024. Using pollen in turbidites for vegetation reconstructions. J. Quat. Sci. 39 (7), 1053–1063.
McGann, M., 2018. Selective transport of palynomorphs in marine turbiditic deposits: An example from the Ascension-Monterey Canyon system offshore central California. Quat. Int. 469, 120–140.
McGlone, M.S., 1985. Plant biogeography and the late Cenozoic history of New Zealand. N. Z. J. Bot. 23 (4), 723–749.
McGlone, M.S., 2001. A late Quaternary pollen record from marine core P69, southeastern North Island, New Zealand. N. Z. J. Geol. Geophys. 44, 69–77.
McGlone, M.S., Howorth, R., Pullar, W., 1984. Late Pleistocene stratigraphy, vegetation and climate of the Bay of Plenty and Gisborne regions, New Zealand. N. Z. J. Geol. Geophys. 27, 327–350.
McGlone, M.S., Newnham, R.M., Moar, N.T., 2010. The vegetation cover of New Zealand during the Last Glacial Maximum: do pollen records under-represent woody vegetation. Terra Aust. 32, 49–68.
McGlone, M.S., Topping, W., 1983. Late Quaternary vegetation, Tongariro region, central North Island, New Zealand. N. Z. J. Bot. 21, 53–76.
Mildenhall, D., 1976. Exotic pollen rain on the Chatham Islands during the late Pleistocene. N. Z. J. Geol. Geophys. 19, 327–333.
Mildenhall, D., 1995. Pleistocene palynology of the Petone and Seaview drillholes, Petone, Lower Hutt Valley, North Island, New Zealand. J. R. Soc. N. Z. 25, 207–262.
Mildenhall, D., 2003. Deep-sea record of Pliocene and Pleistocene terrestrial palynomorphs from offshore eastern New Zealand (ODP Site 1123, Leg 181). N. Z. J. Geol. Geophys. 46, 343–361.
Mildenhall, D., Hollis, C., Naish, T., 2004. Orbitally-influenced vegetation record of the Mid-Pleistocene climate transition, offshore eastern New Zealand (ODP Leg 181, Site 1123). Mar. Geol. 205, 87–111.
Mildenhall, D., Orpin, A., 2010. Terrestrial palynology from marine cores as an indicator of environmental change for the Waipaoa Sedimentary System and north-eastern New Zealand. Mar. Geol. 270, 227–234.
Moar, N.T., et al., 1993. Pollen Grains of New Zealand Dicotyledonous Plants. Manaaki Whenua Press.
Montade, V., Nebout, N.C., Kissel, C., Mulsow, S., 2011. Pollen distribution in marine surface sediments from Chilean Patagonia. Mar. Geol. 282, 161–168.
Moss, P.T., Kershaw, A.P., Grindrod, J., 2005. Pollen transport and deposition in riverine and marine environments within the humid tropics of northeastern Australia. Rev. Palaeobot. Palynol. 134, 55–69.
Mountjoy, J.J., Howarth, J.D., Orpin, A.R., Barnes, P.M., Bowden, D.A., Rowden, A.A., Schimel, A.C., Holden, C., Horgan, H.J., Nodder, S.D., et al., 2018. Earthquakes drive large-scale submarine canyon development and sediment supply to deep-ocean basins. Sci. Adv. 4, eaar3748.
Nakagawa, T., 2007. PolyCounter ver. 1.0 & ergodex DX-1: A cheap and very ergonomic electronic counter board system. Quat. Int. 167, 298.
National Institute of Water and Atmospheric Research (NIWA), 2025. NZ River Maps. Online. https://shiny.niwa.co.nz/nzrivermaps/. (Accessed 08 January 2025).
Nelson, C., Hendy, I., Neil, H., Hendy, C., Weaver, P., 2000. Last glacial jetting of cold waters through the Subtropical Convergence zone in the Southwest Pacific off eastern New Zealand, and some geological implications. Palaeogeogr. Palaeoclimatol. Palaeoecol. 156, 103–121.
Newnham, R., 1992. A 30 000 year pollen, vegetation and climate record from Otakairangi (Hikurangi), Northland, New Zealand. J. Biogeogr. 541–554.

Newnham, R., Alloway, B., 2004. A terrestrial record of last interglacial climate preserved by voluminous debris avalanche inundation in Taranaki, New Zealand. J. Quat. Sci. 19, 299–314.
Newnham, R., Alloway, B., McGlone, M., Juchnowicz, H., Rees, A., Wilmshurst, J., 2017. A last interglacial pollen-temperature reconstruction, central North Island, New Zealand. Quat. Sci. Rev. 170, 136–151.
Newnham, R.M., Lowe, D.J., 2000. Fine-resolution pollen record of late-glacial climate reversal from New Zealand. Geology 28, 759–762.
Newnham, R.M., Lowe, D.J., Giles, T., Alloway, B.V., 2007a. Vegetation and climate of Auckland, New Zealand, since ca. 32 000 cal. yr ago: support for an extended LGM. J. Quat. Sci.: Publ. Quat. Res. Assoc. 22, 517–534.
Newnham, R.M., Lowe, D.J., Williams, P.W., 1999. Quaternary environmental change in New Zealand: a review. Prog. Phys. Geogr. 23, 567–610.
Newnham, R., McGlone, M., Moar, N., Wilmshurst, J., Vandergoes, M., 2013. The vegetation cover of New Zealand at the Last Glacial Maximum. Quat. Sci. Rev. 74, 202–214.
Newnham, R.M., Vandergoes, M.J., Hendy, C.H., Lowe, D.J., Preusser, F., 2007b. A terrestrial palynological record for the last two glacial cycles from southwestern New Zealand. Quat. Sci. Rev. 26, 517–535.
Noda, A., Greve, A., Woodhouse, A., Crundwell, M., 2024. Depositional rate, grain size and magnetic mineral sulfidization in turbidite sequences, Hikurangi Margin, New Zealand. N. Z. J. Geol. Geophys. 67, 288–311.
Orpin, A., 2004. Holocene sediment deposition on the Poverty-slope margin by the muddy Waipaoa River, East Coast New Zealand. Mar. Geol. 209, 69–90.
Pahnke, K., Sachs, J.P., 2006. Sea surface temperatures of southern midlatitudes 0–160 kyr BP. Paleoceanography 21.
Pank, K., Kutterolf, S., Schindlbeck-Belo, J., Hopkins, J.L., Wang, K.L., Lee, H.Y., Schmitt, A.K., 2025. A Quaternary marine tephrostratigraphic record of New Zealand's explosive volcanism–Integration of medial and distal to ultra-distal marine tephra inventories. 446, p. 108404.
Parra, J.G., Marsaglia, K.M., Rivera, K.S., Dawson, S.T., Walsh, J., 2012. Provenance of sand on the Poverty Bay shelf, the link between source and sink sectors of the Waipaoa River sedimentary system. Sediment. Geol. 280, 208–233.
Pedley, K.L., Barnes, P.M., Pettinga, J.R., Lewis, K.B., 2010. Seafloor structural geomorphic evolution of the accretionary frontal wedge in response to seamount subduction, Poverty Indentation, New Zealand. Mar. Geol. 270, 119–138.
Pickering, K.T., Pouderoux, H., McNeill, L.C., Backman, J., Chemale, F., Kutterolf, S., Milliken, K.L., Mukoyoshi, H., Henstock, T.J., Stevens, D.E., et al., 2020. Sedimentology, stratigraphy and architecture of the Nicobar Fan (Bengal–Nicobar Fan System), Indian Ocean: results from International Ocean Discovery Program Expedition 362. Sedimentology 67, 2248–2281.
Piper, D.J., Normark, W.R., 2009. Processes that initiate turbidity currents and their influence on turbidites: A marine geology perspective. J. Sediment. Res. 79, 347–362.
Piva, S.B., Barker, S.J., Newnham, R.M., Rees, A.B., Wilson, C.J., Carter, L., Iverson, N.A., Läuchli, B., Augustinus, P.C., 2023. Millimetre-scale pollen analysis of non-varved lacustrine sediments from Onepoto maar palaeolake, Auckland, reveals distal vegetation responses and landscape recovery following the ~25.5-ka Ōruanui supereruption. J. Quat. Sci. 38, 613–628.
Plew, D.R., Zeldis, J.R., Shankar, U., Elliott, A.H., 2018. Using simple dilution models to predict New Zealand estuarine water quality. Estuaries Coasts 41, 1643–1659.
Pocknall, D.T., 1981a. Pollen morphology of the New Zealand species of Dacrydium Selander, Podocarpus L'Heritier, and Dacrycarpus Endlicher (Podocarpaceae). N. Z. J. Bot. 19, 67–95.
Pocknall, D.T., 1981b. Pollen morphology of the New Zealand species of Libocedrus endlicher (Cupressaceae) and Agathis salisbury (Araucariaceae). N. Z. J. Bot. 19, 267–272.
Pocknall, D.T., 1981c. Pollen morphology of Phyllocladus L.C. et A. Rich. N. Z. J. Bot. 19, 259–266.
Pouderoux, H., Lamarche, G., Proust, J.N., 2012b. Building an 18 000-year-long paleoearthquake record from detailed deep-sea turbidite characterisation in Poverty Bay, New Zealand. Nat. Hazards Earth Syst. Sci. 12, 2077–2101.
Pouderoux, H., Proust, J.N., Lamarche, G., Orpin, A., Neil, H., 2012a. Postglacial (after 18 ka) deep-sea sedimentation along the Hikurangi Subduction Margin (New Zealand): Characterisation, timing and origin of turbidites. Mar. Geol. 295, 51–76.
Ryan, M., Dunbar, G., Vandergoes, M., Neil, H., Hannah, M., Newnham, R., Bostock, H., Alloway, B., 2012. Vegetation and climate in Southern Hemisphere mid-latitudes since 210 ka: new insights from marine and terrestrial pollen records from New Zealand. Quat. Sci. Rev. 48, 80–98.
Ryan, M.T., Newnham, R.M., Dunbar, G.B., Vandergoes, M.J., Rees, A.B., Neil, H., Callard, S.L., Alloway, B.V., Bostock, H., Hua, Q., et al., 2016. Exploring the source-to-sink residence time of terrestrial pollen deposited offshore Westland, New Zealand. Rev. Palaeobot. Palynol. 230, 37–46.
Saffer, D., Wallace, L., Barnes, P., Pecher, I., Petronotis, K., LeVay, L., Bell, R., Crundwell, M., Oliveira, C.Engelmann.de., Fagereng, A., et al., 2019. Expedition 372b/375 summary. In: Proceedings of the International Ocean Discovery Program. IODP., pp. 1–35.
Sánchez-Goñi, M.F., Desprat, S., Fletcher, W.J., Morales-Molino, C., Naughton, F., Oliveira, D., Urrego, D.H., Zorzi, C., 2018. Pollen from the deep-sea: A breakthrough in the mystery of the Ice Ages. Front. Plant Sci. 9 (38).
Sánchez-Goñi, M.F., Llave, E., Oliveira, D., Naughton, F., Desprat, S., Ducassou, E., Hodell, D., Hernandez-Molina, F.J., 2016. Climate changes in south western Iberia and Mediterranean Outflow variations during two contrasting cycles of the last 1 Myrs: MIS 31–MIS 30 and MIS 12–MIS 11. Glob. Planet. Change 136, 18–29.
Schaefer, G., Rodger, J.S., Hayward, B.W., Kennett, J.P., Sabaa, A.T., Scott, G.H., 2005. Planktic foraminiferal and sea surface temperature record during the last 1 Myr across the Subtropical Front, Southwest Pacific. Mar. Micropaleontol. 54, 191–212.
Schindler, J., Dymond, J.R., Wiser, S.K., Shepherd, J.D., 2021. Method for national mapping spatial extent of southern beech forest using temporal spectral signatures. Int. J. Appl. Earth Obs. Geoinf. 102, 102408.
Scott, L., van Zinderen Barker Sr, E.M., 1985. Exotic pollen and long-distance wind dispersal at a sub-antarctic island. Grana 24, 45–54.
Shorrock, A.E., Strachan, L.J., Barnes, P.M., Moore, G.F., McArthur, A.D., Gamboa, D., Woodhouse, A.D., Bell, R.E., Davidson, S.R., Bostock, H.C., 2025. Coeval Transverse and Axial Sediment Delivery to the Northern Hikurangi Trough During the Late Quaternary. Basin Research 37 (1), e70019.
Shulmeister, J., Shane, P., Lian, O.B., Okuda, M., Carter, J.A., Harper, M., Dickinson, W., Augustinus, P., Heijnis, H., 2001. A long late-Quaternary record from lake Poukawa, Hawke's Bay, New Zealand. Palaeogeogr. Palaeoclimatol. Palaeoecol. 176, 81–107.
Spratt, R.M., Lisiecki, L.E., 2016. A Late Pleistocene sea level stack. Clim. the Past 12, 1079–1092.
Star, P., 2008. Tree planting in Canterbury, New Zealand, 1850-1910. Environ. Hist. 14, 563–582.
Stevens, C.L., O'Callaghan, J.M., Chiswell, S.M., Hadfield, M.G., 2021. Physical oceanography of New Zealand/Aotearoa shelf seas–a review. N. Z. J. Mar. Freshw. Res. 55 (1), 6–45.
Stewart, R., Neall, V., 1984. Chronology of palaeoclimatic change at the end of the last glaciation. Nature 311, 47–48.
Stockmarr, J., 1971. Tables with spores used in absolute pollen analysis. Pollen et Spores 13, 615–621.
Talling, P.J., Baker, M.L., Pope, E.L., Ruffell, S.C., Jacinto, R.S., Heijnen, M.S., Hage, S., Simmons, S.M., Hasenhündl, M., Heerema, C.J., et al., 2022. Longest sediment flows yet measured show how major rivers connect efficiently to deep sea. Nat. Commun. 13 (4193).
Talling, P.J., Masson, D.G., Sumner, E.J., Malgesini, G., 2012. Subaqueous sediment density flows: Depositional processes and deposit types. Sedimentology 59, 1937–2003.
Talling, P.J., Paull, C.K., Piper, D.J., 2013. How are subaqueous sediment density flows triggered, what is their internal structure and how does it evolve? direct observations from monitoring of active flows. Earth-Sci. Rev. 125, 244–287.
Tek, D.E., McArthur, A.D., Poyatos-Moré, M., Colombera, L., Allen, C., Patacci, M., McCaffrey, W.D., 2022. Controls on the architectural evolution of deep-water channel overbank sediment wave fields: insights from the Hikurangi Channel, offshore New Zealand. N. Z. J. Geol. Geophys. 65, 141–178.
Tomlinson, P., 1994. Functional morphology of saccate pollen in conifers with special reference to Podocarpaceae. Int. J. Plant Sci. 155, 699–715.
Trewick, S., Bland, K., 2012. Fire and slice: palaeogeography for biogeography at New Zealand's North Island/South Island juncture. J. R. Soc. N. Z. 42, 153–183.
Underwood, M.B., 2022. Composition of fine-grained sediment in the Hikurangi Trough: Evidence for intermingling among axial gravity flows, transverse gravity flows and margin-parallel ocean currents. Sedimentology 70, 828–864.
Underwood, M.B., Hoke, K.D., Fisher, A.T., Davis, E.E., Giambalvo, E., Zühlsdorff, L., Spinelli, G.A., 2005. Provenance, stratigraphic architecture, and hydrogeologic influence of turbidites on the mid-ocean ridge flank of northwestern Cascadia Basin, Pacific Ocean. J. Sediment. Res. 75, 149–164.
Underwood, M.B., Pickering, K.T., 2018. Facies architecture, detrital provenance, and tectonic modulation of sedimentation in the Shikoku Basin: Inputs to the Nankai Trough subduction zone. In: Kimura, G. (Ed.), Geology and Tectonics of Subduction Zones: A Tribute To Gaku Kimura. Geological Society of America. In: Geological Society of America Special Papers, vol. 534, pp. 1–20. http://dx.doi.org/10.1130/2018.2534(01).
Upton, P., Kettner, A.J., Gomez, B., Orpin, A.R., Litchfield, N., Page, M.J., 2013. Simulating post-LGM riverine fluxes to the coastal zone: The Waipaoa River System, New Zealand. Comput. Geosci. 53, 48–57.
van den Bos, V., Newnham, R., Rees, A., Woods, L., 2020. Density separation in pollen preparation: How low can you go? J. Paleolimnol. 63, 225–234.
Vandergoes, M.J., Newnham, R.M., Denton, G.H., Blaauw, M., Barrell, D.J., 2013. The anatomy of Last Glacial Maximum climate variations in south Westland, New Zealand, derived from pollen records. Quat. Sci. Rev. 74, 215–229.
Vandergoes, M.J., Newnham, R.M., Preusser, F., Hendy, C.H., Lowell, T.V., Fitzsimons, S.J., Hogg, A.G., Kasper, H.U., Schlüchter, C., 2005. Regional insolation forcing of late Quaternary climate change in the Southern Hemisphere. Nature 436, 242–245.
Vieira, M., Jolley, D., 2020. Stratigraphic and spatial distribution of palynomorphs in deep-water turbidites: A meta-data study from the UK Central North Sea Paleogene. Mar. Pet. Geol. 122, 104638.
Walker, S., Price, R., Rutledge, D., Stephens, T., Lee, W., 2006. Recent loss of indigenous cover in New Zealand. N. Z. J. Ecol..

Wallace, L.M., Reyners, M., Cochran, U., Bannister, S., Barnes, P.M., Berryman, K., Downes, G., Eberhart-Phillips, D., Fagereng, A., Ellis, S., et al., 2009. Characterizing the seismogenic zone of a major plate boundary subduction thrust: Hikurangi Margin, New Zealand. Geochem. Geophys. Geosystems 10.

Wardle, P, 1991. Vegetation of New Zealand. CUP Archive.

Weaver, P.P., Carter, L., Neil, H.L., 1998. Response of surface water masses and circulation to late Quaternary climate change east of New Zealand. Paleoceanography 13, 70–83.

Weedon, G.P., Hall, I.R., 2004. Neogene palaeoceanography of Chatham Rise (Southwest Pacific) based on sediment geochemistry. Mar. Geol. 205, 207–225.

Wilmshurst, J.M., 1997. The impact of human settlement on vegetation and soil stability in Hawke's bay, New Zealand. N. Z. J. Bot. 35, 97–111.

Wilmshurst, J.M., Anderson, A.J., Higham, T.F., Worthy, T.H., 2008. Dating the late prehistoric dispersal of Polynesians to New Zealand using the commensal Pacific rat. Proc. Natl. Acad. Sci. 105, 7676–7680.

Wilmshurst, J.M., Eden, D.N., Froggatt, P.C., 1999. Late Holocene forest disturbance in Gisborne, New Zealand: A comparison of terrestrial and marine pollen records. N. Z. J. Bot. 37, 523–540.

Wood, J., Wilmshurst, J., Newnham, R., McGlone, M., 2017. Evolution and ecological change during the New Zealand Quaternary. Landsc. Quat. Environ. Chang. N. Z. 23, 5–291.

Woodhouse, A., Barnes, P.M., Shorrock, A., Strachan, L.J., Crundwell, M., Bostock, H.C., Hopkins, J., Kutterolf, S., Pank, K., Behrens, E., et al., 2024. Trench floor depositional response to glacio-eustatic changes over the last 45 ka, northern Hikurangi subduction margin, New Zealand. N. Z. J. Geol. Geophys. 67, 312–335.

Wright, I.C., McGlone, M.S., Nelson, C.S., Pillans, B.J., 1995. An integrated latest Quaternary (Stage 3 to present) paleoclimatic and paleoceanographic record from offshore northern New Zealand. Quat. Res. 44, 283–293.

Zhu, Y., Xie, Y., Cheng, B., Chen, F., Zhang, J., 2003. Pollen transport in the Shiyang River drainage, arid China. Chin. Sci. Bull. 48, 1499–1506.

Zwier, M., van der Bilt, W.G., de Stigter, H., Bjune, A.E., 2022. Pollen evidence of variations in Holocene climate and Southern Hemisphere Westerly Wind strength on sub-Antarctic South Georgia. Holocene 32, 147–158.